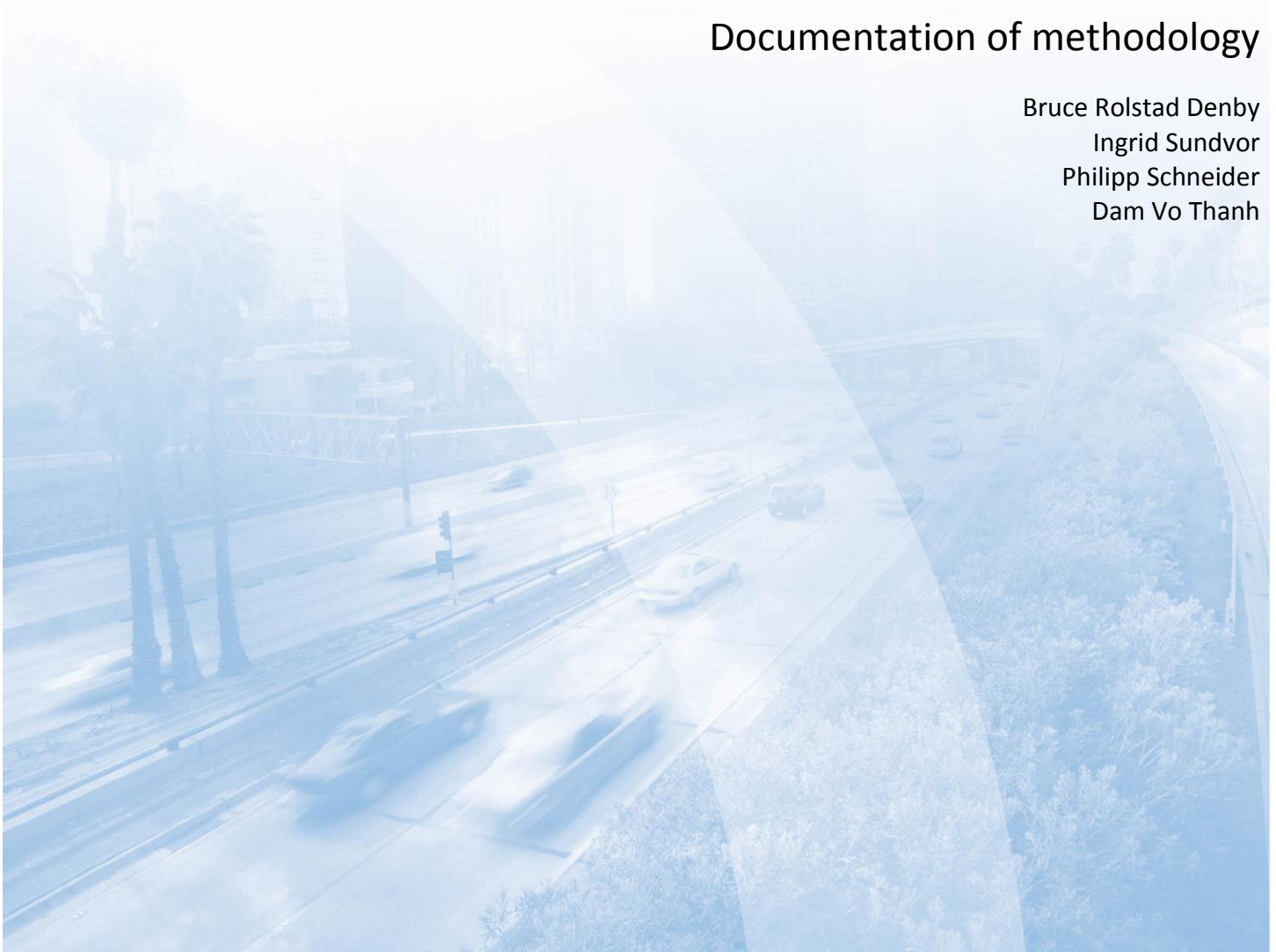

Air quality maps of NO₂ and PM₁₀ for the region including Stavanger, Sandnes, Randaberg and Sola (Nord-Jæren)

Documentation of methodology

Bruce Rolstad Denby
Ingrid Sundvor
Philipp Schneider
Dam Vo Thanh



Technical report

Preface

This technical report provides detailed documentation (in English) of the air quality modelling and mapping activities carried out to create maps of PM₁₀ and NO₂ in the Nord-Jæren region. This documentation supports the summary report (in Norwegian) provided to Statens Vegvesen region west (NILU report 57/2013) entitled 'Luftkvalitetskart av NO₂ og PM₁₀ for byområdet Stavanger, Sandnes, Randaberg og Sola (Nord-Jæren): oppsummeringsrapport'. This technical report is intended to provide background information for the summary report and to provide internal documentation for the methodology used.

Contents

	Page
Preface	1
Contents	3
1 Introduction and background	5
2 Emissions	6
2.1 Area emissions	7
2.2 Domestic wood burning emissions, temperature dependence and spatial distribution	10
2.3 Traffic data	12
2.4 Traffic exhaust emissions and congestion parameterisation	14
2.5 Traffic non- exhaust emissions (NORTRIP).....	16
3 Modelling	20
3.1 Meteorological data and modelling.....	21
3.2 Regional background concentrations	23
3.3 NO ₂ chemistry parameterisation	24
4 Analysis of measurements	25
4.1 Offset in NO ₂ and NO _x measurements	25
4.2 Ratio of NO ₂ and NO _x	26
4.3 Ratio of PM _{2.5} and PM ₁₀	27
5 Validation	28
5.1 NO ₂	28
5.2 O ₃	29
5.3 NO _x	31
5.4 PM ₁₀	32
5.5 PM _{2.5}	34
6 Modelled source apportionment	36
6.1 NO _x source contribution and temporal variability	36
6.2 PM ₁₀ source contribution and temporal variability	37
7 Mapping method and maps	38
7.1 Mapping receptors and post processing	38
7.2 Final maps of NO ₂	42
7.3 Final maps of PM ₁₀	45
8 Recommendations and improvements	48
8.1 Area emissions	48
8.2 Traffic data	49
8.3 NORTRIP modelling.....	49
8.4 NO ₂ chemistry parameterisation	49
8.5 Mapping	50
8.6 Meteorology	50
8.7 Air quality measurements.....	50
9 References	51

Air quality maps of NO₂ and PM₁₀ for the region including Stavanger, Sandnes, Randaberg and Sola (Nord-Jæren)

Documentation of methodology

1 Introduction and background

This report provides detailed background documentation of the air quality modelling and mapping activities carried out at NILU for the mapping of PM₁₀ and NO₂ in the Nord-Jæren region. This documentation supports the ‘summary report’ (in Norwegian) provided to Statens Vegvesen region west (NILU report TR 57/2013) entitled ‘Luftkvalitetskart av NO₂ og PM₁₀ for byområdet Stavanger, Sandnes, Randaberg og Sola (Nord-Jæren): oppsummeringsrapport’.

This report provides both background information for the summary report as well as providing internal documentation for the methodologies used. Good knowledge of air quality modelling is required in order to understand much of the description, though there are a large number of supporting figures that are self-explanatory.

Most modelling and mapping activities in the urban environment are carried out at NILU using AirQUIS (www.airquis.com), a comprehensive air quality management system that includes measurement and emission databases as well as modelling, analysis and presentation tools. However, AirQUIS is designed for specific types of applications and is limited in the ways it can both model and present data. As a result any application requiring alternative inputs or results must be carried out external to AirQUIS. This is the case for this particular application, the mapping of air quality in the Nord-Jæren region. Requirements concerning the mapping resolution and form as well as the use of state-of-the-science road dust emission models means that the emissions, model input data, model output, presentation and analysis are all carried out within the MATLAB programming environment for which a suite of codes have been developed.

Despite the differences in ‘packaging’ both AirQUIS and this current application use the same air quality model, the EPISODE model (Slørdal et al., 2003), which has been successfully applied on a large range of applications. Because of the non-standard nature of this application this documentation report has been written to describe the methodology applied and to present results in more detail than are given in the ‘Summary report’ of the results.

The model application and domain is the Nord-Jæren peninsula containing the municipalities of Stavanger, Sandnes, Randaberg and Sola. This same region is currently modelled using AirQUIS as part of the Better City Air (Bedre Byluft) forecasting system (Bedre byluft, 2013; Ødegaard et al., 2013). As such emissions inventories and other model input data already exist and are used as a starting point for the modelling and mapping. The model region is shown in Figure 1.

The maps to be created are required at 100 m resolution for the entire model domain and are to present annual mean concentrations of PM₁₀ and NO₂ as well as

the percentile concentrations corresponding to the 19'th highest hourly mean NO₂ concentrations and the 36'th highest PM₁₀ daily mean concentrations. These maps are thus directly related to the European and national Air Quality Directives. For a description of these see the summary report.

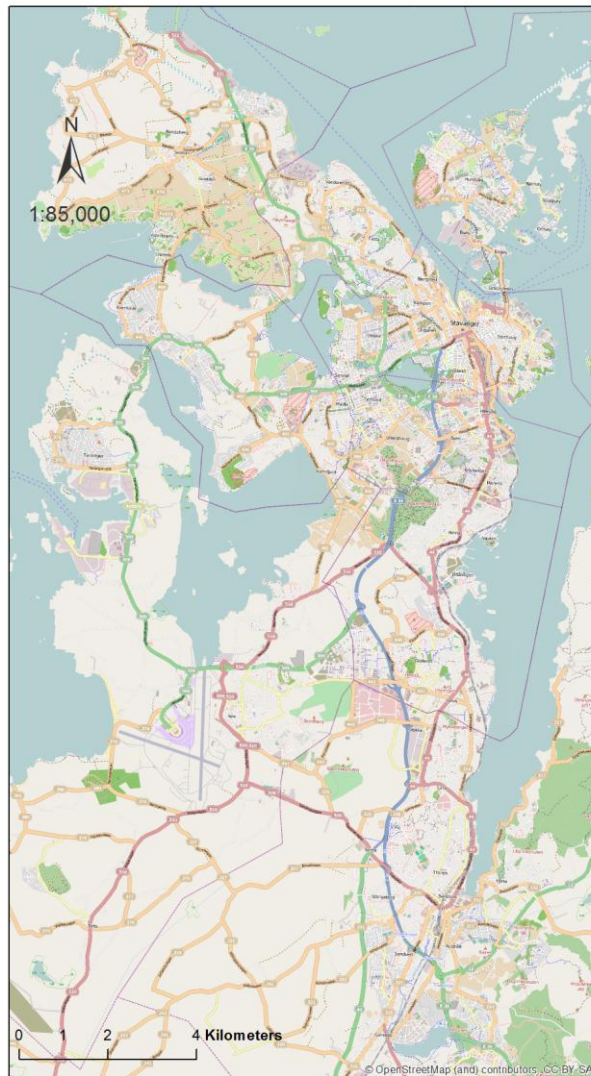


Figure 1. Model domain extracted from the 'open street map software' using ArcGIS software, also used to visualise the final maps.

2 Emissions

The model and emissions are divided into two different types. The first are 'area' emissions, such as heating and shipping, that are distributed diffusely in space. The second type are 'line source' emissions that are exclusively related to traffic emissions from roads. In the model these two sorts of emissions are dealt with in two different ways.

In the project call and tendered proposal description it was indicated that emissions inventories were to be taken 'as is' as updating of the current emissions database would have required far more time and resources than were available. To a large extent the existing emissions have been used but some exceptions have

been made and the following ‘changes’ to the existing database have been included.

- The NORTRIP road dust emission model has been used to calculate non-exhaust traffic emissions.
- A congestion parameterisation has been included for calculation of hourly levels of congestion and traffic speed. This allows for traffic congestion and speed to vary from hour to hour and is applied to determine the traffic exhaust emissions factors and the traffic speed required by NORTRIP to determine road wear and suspension.
- Domestic heating has been redistributed in both space and time whilst retaining the same existing total emissions for the model region. Redistribution in time is based on observed average weekly temperature and redistribution in space is based on the density of dwellings.

The total emissions are shown below in Table 1. The same as in Table 2 in the summary report

Table 1: Total emissions (ton/year) of PM₁₀ and NO_x within the model domain.

Source	Type of emission	PM ₁₀ (ton/year)	NO _x (ton/year)
Domestic wood burning	Area	307	63
Diverse industry	Area	6.7	78
Commercial heating and other	Area	2.7	42
Non-wood Heating	Area	0.9	15
Mobile combustion sources	Area	20	164
Ship and railway	Area	9.6	921
Air traffic and airports	Area	2.6	58
Traffic exhaust	Line	63	1928
Traffic non-exhaust	Line	233	0
Total		645.5	3269

2.1 Area emissions

All area emissions are calculated using the MATLAB emission scripts. These scripts read in AirQUIS excel templates and produce emission files in gridded format suitable for running in EPISODE. Area emissions are provided in these excel templates per ‘grunnkrets’ (the smallest administrative area) or some other regional polygon data with a reference ID. These emissions were originally provided by Statistisk sentralbyrå (SSB). Many of these emissions are well over a decade old and an extensive assessment of their validity has never been carried out.

Shape files are used to define the spatial co-ordinates of the emission polygons. The MATLAB routines take the polygons and redistribute the emissions to the model grid, as in AirQUIS. This means that the resolution of the emissions data is not per grid but per polygon. This can lead to a poor distribution of the area emissions. For example shipping emissions, that are specific in space but are included in a larger polygon ‘grunnkrets’, may be distributed over land in the grid, which is of course unrealistic. The same is true for land based emissions, such as

wood burning, that can have contributions over the sea, also very unrealistic. Though no changes were made in the shipping emissions the domestic heating emissions were redistributed, see Section 2.2, to avoid this error.

All area emissions are placed in the model grid as either ‘lower level’ emissions (lowest level grid only), such as mobile combustion sources and airport emissions, or as ‘upper level emissions’ (second and third model grid layers), such as heating and shipping.

Table 1 indicates all the area emissions that are included in the calculations for PM_{10} and NO_x . In Figure 2 and Figure 3 we show the spatial and temporal distribution of these area emissions, both upper and lower levels. The PM_{10} area emissions are dominated by domestic heating from wood burning, see section 2.2, whilst those for NO_x are largely due to shipping.

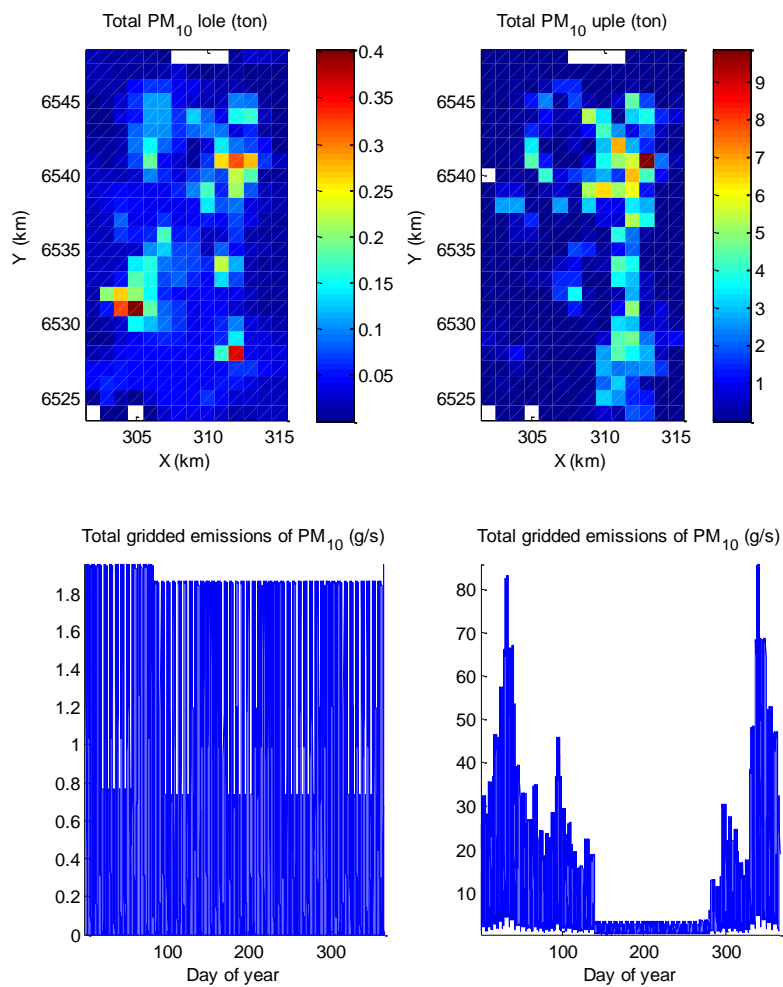


Figure 2. Total area emissions for PM_{10} used in the modelling. Left is lower level and right is upper level emissions.

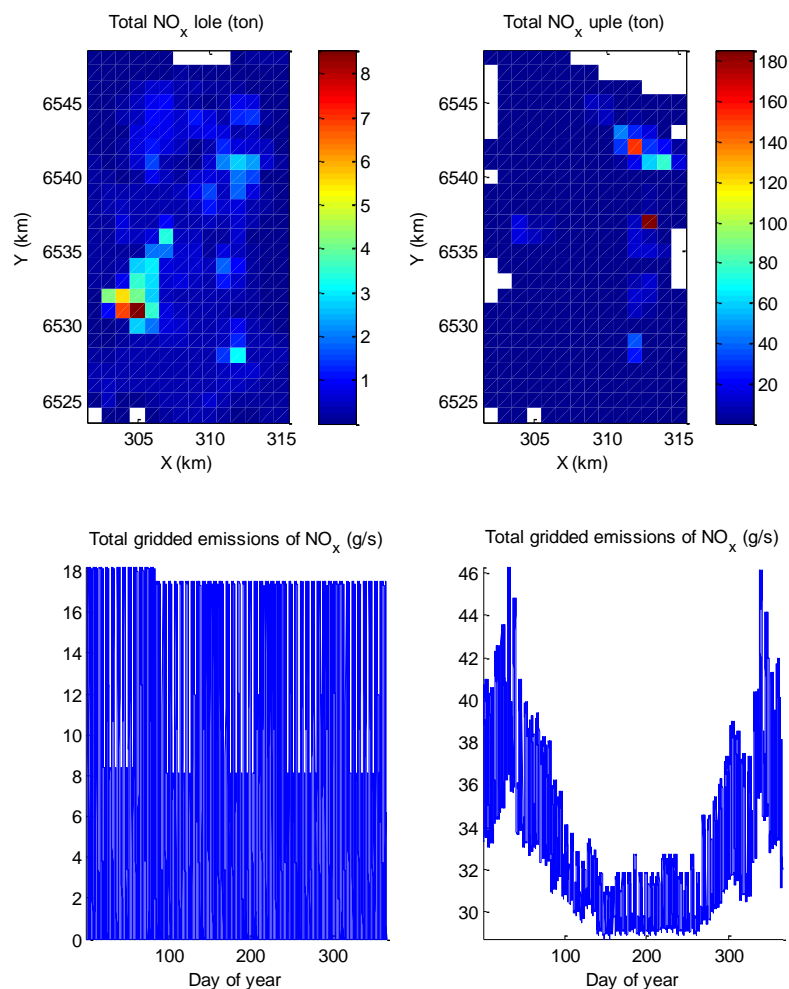


Figure 3. Total area emissions of NO_x used in the modelling. Left is lower level and right is upper level emissions.

The NO_x emissions for shipping are shown separately in Figure 4. As previously commented these shipping emissions are not well distributed over the sea or port areas due to the fact that emissions are provided in ‘grunnkrets’ polygons and also possibly due to other distribution errors. The highest gridded emissions, at 313 km E and 3537 km N, do not appear to be correctly positioned either. Comparison of the final concentration maps for NO₂ with the underlying land use coverage indicate these high shipping emissions to be over a shopping centre. A port region lies 2 km to the south but it is not known if this is the intended source of these emissions. No further investigation was carried out to find the cause of these discrepancies.

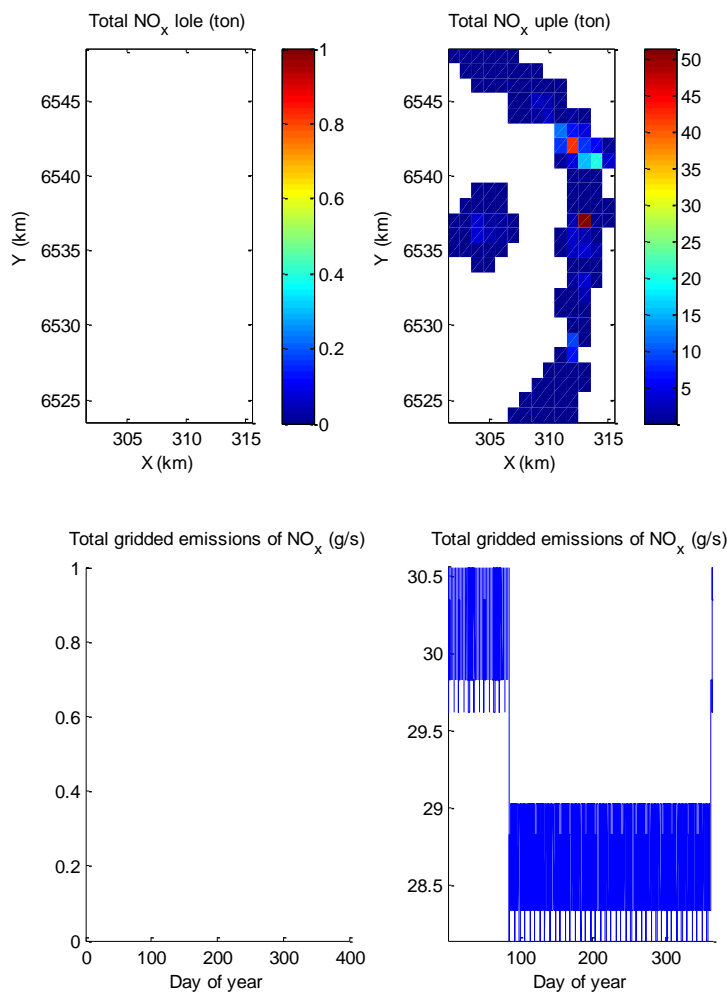


Figure 4. Area emissions of NO_x for shipping in the model domain. Shipping is placed as an upper level area emission and so there is no contribution to the lower level emissions (left).

2.2 Domestic wood burning emissions, temperature dependence and spatial distribution

Due to the poor distribution of the domestic wood burning emissions and their relative importance it was decided to redistribute these emissions according to the density of dwellings directly within the model grid, instead of using the polygon ‘grunnkrets’ as basis for the distribution. Home address data for the Nord-Jæren region was used, which is part of the AirQUIS database in Bedre Byluft.

In addition to the spatial distribution of the domestic wood burning the temporal distribution was also altered. In the original AirQUIS emission database domestic heating was either ‘on’ in winter or ‘off’ in summer, with daily and weekday variability. This ‘on/off’ seasonal distribution was considered to be a poor temporal distribution for domestic heating. Instead, the weekly mean temperature was used together with a parameterisation to distribute the emissions in time. A similar method has been applied in Oslo for PM_{10} calculations (Denby, 2013;

Denby and Sundvor, 2013). This method sets the ‘week of year’ temporal emission variation factor for each week (`weekly_factor_wood`) according to the following formulation, taken directly from the MATLAB code.

```
weekly_factor_wood=factor_max-(T_st_weekly-T_min)/(T_max-
T_min)*(factor_max-factor_min);
```

bounded by

```
weekly_factor_wood=max(factor_min,weekly_factor_wood);
weekly_factor_wood=min(factor_max,weekly_factor_wood);
```

where

```
T_max=10;T_min=-10;factor_max=0.04;factor_min=0.001;
```

and `T_st_weekly` is the average weekly temperature.

This formulation increases the weekly factor from a minimum value (`factor_min`) to a maximum value (`factor_max`) linearly with decreasing temperature. The minimum temperature is set at -10 and the maximum at 10 °C. In the Nord-Jæren application this weekly factor was normalised so that the total domestic heating emissions are equal to the total emissions provided by SSB.

```
weekly_factor_wood=weekly_factor_wood/sum(weekly_factor_wood);
```

The resulting spatial and temporal emissions are shown, along with the original wood burning emissions, in Figure 5. These emissions are very similar to the total PM₁₀ emissions in Figure 2 since it is the domestic heating that dominates the PM₁₀ emissions.

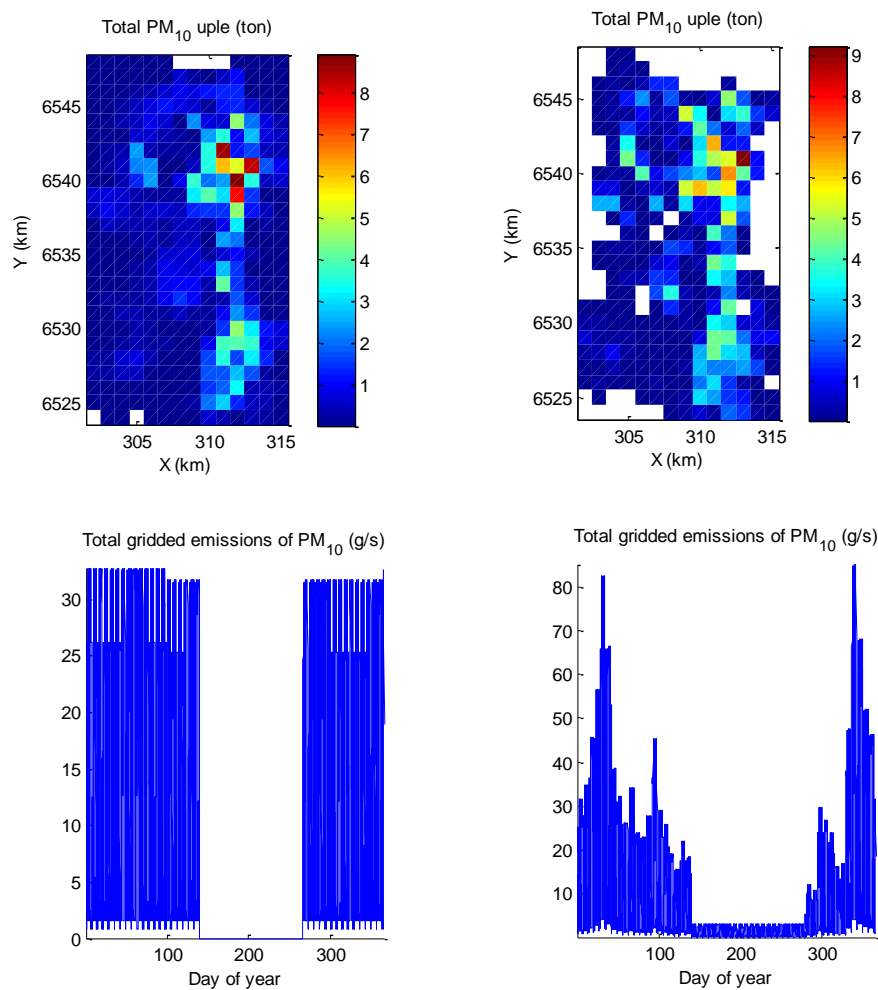


Figure 5. Area emissions for PM_{10} from domestic wood burning only. Left is the original spatial and temporal distribution, right is the temperature dependent and dwelling density dependent emissions used in the modelling.

2.3 Traffic data

For each road link the position of the road nodes, the ADT (Average daily traffic), the fraction of heavy duty vehicles (HDV), the speed limit, the slope (set to 0 in this application), the road type (Highway, tunnel, communal, etc.) and the road width is provided. These road link data, contained in AirQUIS excel templates and extracted from the NVDB database (Statens vegvesen, 2013), are coupled to road link shape files that provide a more detailed description of the shape of the roads. The excel data consists of 13 264 road links and when coupled to the road shape data this increases to 17 888 individual road links in total. All these were taken from the existing Bedre Byluft database in AirQUIS for the Nord-Jæren region which was updated from NVDB in 2012.

A selection process is carried out so that only roads with $ADT > 1000$ veh/day are included as road link emissions (3 342) for the model. The rest of the road links are placed as area emissions in the model. The total emissions from roads with

ADT < 1000 accounts for only 5% of the total traffic emissions. The distribution of all roads are shown in Figure 6.

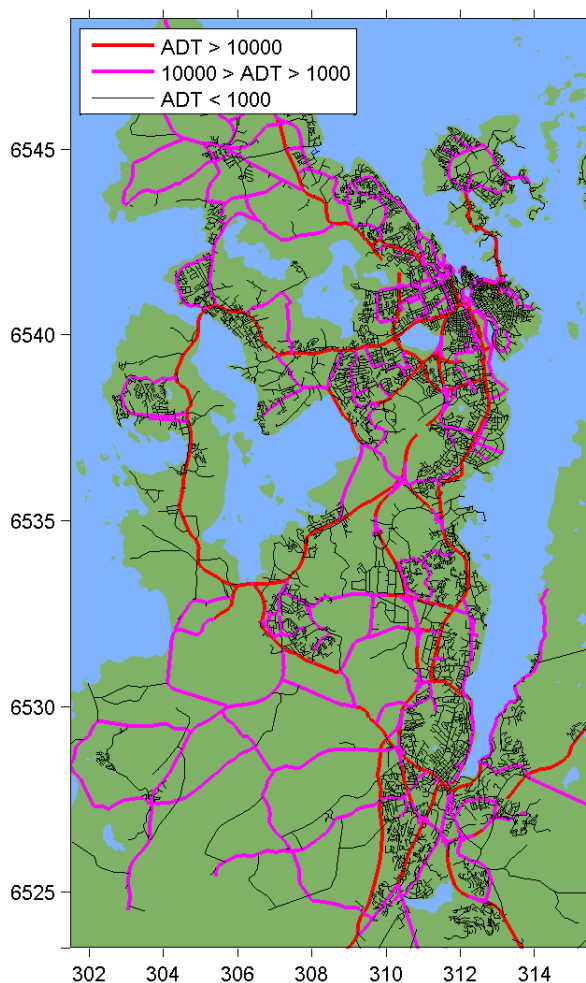


Figure 6: Road link data coupled with shape file data for the Nord-Jæren modelling region. Only roads in red or magenta (ADT > 1000 veh/day) are used directly as line sources in the model calculations.

Tunnels are included in the traffic road data. Their emissions are represented by ‘jets’ at each tunnel entrance. These ‘jets’ are 60 m long road links containing half of the emissions that would result from the traffic passing through the tunnel.

For this application only one daily temporal profile for traffic was used, which was the equivalent of highway temporal profile for Oslo. This profile was most likely not appropriate for most of Nord-Jæren. A request was made to Statens vegvesen for measured traffic data, in order to provide better traffic data for the modelling, but the data was received too late to be included in the calculations. This can be incorporated in any further application.

2.4 Traffic exhaust emissions and congestion parameterisation

Traffic exhaust emissions are calculated using the MATLAB scripts in a similar way as in AirQUIS. Excel templates providing emission factors (driving cycle dependent), vehicle fleet makeup (OFV, 2013), age of vehicles, etc. are used. Different to AirQUIS a congestion parameterisation is applied, instead of using signed speed limits, to determine the appropriate emission factor. NILU has been provided, by TØI (Transportøkonomisk institutt, www.toi.no), emission factors derived from HBEFA (Handbook Emission Factors for Road Transport, www.hbefa.net) for three driving cycles interpreted to be ‘free flow highway’, ‘free flow urban’ and ‘congested flow urban’. These emission factors can vary by a factor of 2 to 3 so assigning the correct driving cycle to each road is relatively important.

In order to determine the appropriate driving cycle a ‘congestion parameterisation’, initially developed by Denby and Sundvor (2013) for Oslo, has also been applied here. In this case the limits of the congestion have been changed due to the different traffic flow conditions found in the Stavanger central region compared to Oslo access roads for which the parameterisation was first derived. The parameterisation uses the average hourly traffic volume per lane (AHT) as input. AHT is determined simply by taking the hourly traffic volume per road link, calculated using the ADT and the temporal traffic profiles for each road, and dividing by the number of lanes, derived from the road width. The parameterised emission factor (EF_{param}) is calculated based on a linear interpolation between the urban free flow and urban congestion emission factors for non-highway roads. For highways the transition from highway free flow and urban free flow is used.

For non-highways the transition between urban free flow emission factors ($EF_{freeflow}$) and urban congested flow emission factors ($EF_{congest}$) occurs according to:

$$\beta = \frac{(AHT - AHT_{min})}{(AHT_{max} - AHT_{min})} \quad \text{for } AHT_{min} < AHT < AHT_{max}$$

$$\beta = 0 \quad \text{for } AHT < AHT_{min}$$

$$\beta = 1 \quad \text{for } AHT > AHT_{max}$$

and

$$EF_{param} = EF_{congest} \cdot \beta + EF_{freeflow} \cdot (1 - \beta)$$

where the AHT limits are set to

$$AHT_{min} = 250 \text{ and } AHT_{max} = 500$$

A similar parameterisation is also used for the transition on highways, with speed limits ≥ 80 km/hr, from urban free flow to highway free flow using AHT limits of

$$AHT_{min} = 0 \text{ and } AHT_{max} = 750$$

Closely related to this parameterisation is a similar parameterisation that calculates average hourly vehicle speed. This is described in Denby and Sundvor (2013).

An example of the impact of the congestion parameterisation is provided in Figure 7 where two roads are shown. These are Madlaveien, a heavily trafficked road next to the Kannik measurement station, and the E39 between Stavanger and Sandnes, a major highway. The average emission factors and speeds are summarised in Table 2. The most significant conclusion to be drawn from these results is that the average EF on Madlaveien is significantly higher (around 30%) when using the congestion parameterisation compared to the default urban free flow $EF_{freeflow}$ and that the highway emission factor is slightly lower (around 12%). The result is that even though total traffic on Madlaveien is lower than on the E39 the total emissions are higher.

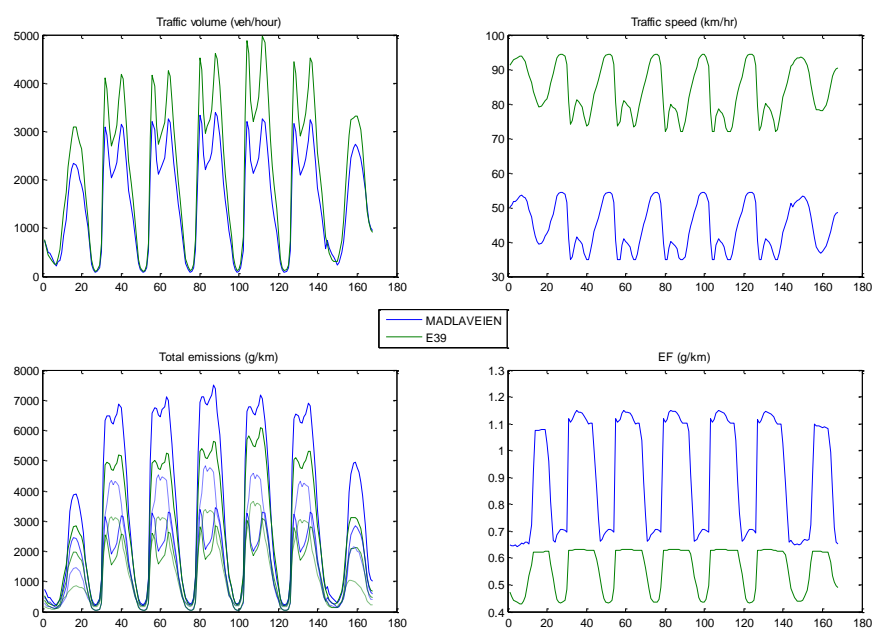


Figure 7: Traffic data and NO_x emissions for the two roads Madlaveien and E39 for a one week period starting on a Sunday. Top left: Hourly total traffic volume. Top right: Traffic speed according to the congestion parameterisation. Bottom left: Hourly emissions of NO_x (solid lines total, dotted lines HDV, dashed lines LDV). Bottom right: Hourly emission factor according to the congestion parameterisation.

Table 2: List of emission factors derived with and without the congestion parameterisation.

	Madlaveien in Kannik	E39 between Stavanger and Sandnes
Emission factors without congestion parameterisation*		
NO _x EF (g/veh/km)	0.67	0.63
NO ₂ EF (g/veh /km)	0.089	0.086
EP** EF (g/veh/km)	0.022	0.021
Emission factors with congestion parameterisation		
NO _x EF (g/veh/km)	0.94	0.56
NO ₂ EF (g/veh/km)	0.122	0.077
EP** EF (g/veh/km)	0.030	0.019
Speed and traffic volume		
Speed limit (km/hr)	50	90
Congestion parameterisation speed (km/hr)	44	84
ADT (veh/day)	38 500	52 000

* Urban free flow emission factors

** Exhaust Particles (EP)

The functionalities associated with this parameterisation are based on Oslo traffic conditions and should in the future be re-analysed using traffic counts from Nord-Jæren.

2.5 Traffic non- exhaust emissions (NORTRIP)

The NORTRIP road dust emission model (Denby and Sundvor, 2012; Denby et al, 2013a; Denby et al., 2013b) has been applied to calculate the non-exhaust emissions from traffic. This model provides the best method for predicting non-exhaust emissions related to road wear using studded tires and is essential for determining the road dust emissions.

In the application for Nord-Jæren the NORTRIP model has been applied in two ways. In the first case the complete model has been applied as a standalone application for Kannik. In the second case the model is applied in simplified form for all roads. In both cases the studded tire share is 28% for passenger and LDV and is 14% for HDV. The studded tire season starts in November and ends mid-April.

2.5.1 Application of the standalone NORTRIP model

In the first case the complete NORTRIP model has been applied at Kannik (Madlaveien) to assess just the emission from this single road. When applying the model in this way it is necessary to use measured NO_x concentrations and estimated NO_x emissions in order to calculate the dispersion, as there is no dispersion model connected to the stand alone version of NORTRIP. In addition urban background concentrations must also be subtracted to compare the model with observed local road contribution. Since both PM₁₀ and NO_x are measured and both Kannik and the nearby urban background station of Våland, all the necessary data are available for calculating concentrations at the Kannik site. Road salting is determined using the inbuilt salting model. Applying the model in

this way provides the best test of the model itself and will indicate how well the model performs given the available meteorological data.

Results of the model calculations at Kannik are shown in Figure 8. The model predicts very well this period, slightly overestimating the mean concentrations by around 15%. The daily mean correlation (R^2) is found to be 0.66. Compared to other applications of NORTRIP (Denby et al., 2013b) this is an above average correlation indicating that the model successfully represents both the road dust emissions and the surface moisture conditions of this road.

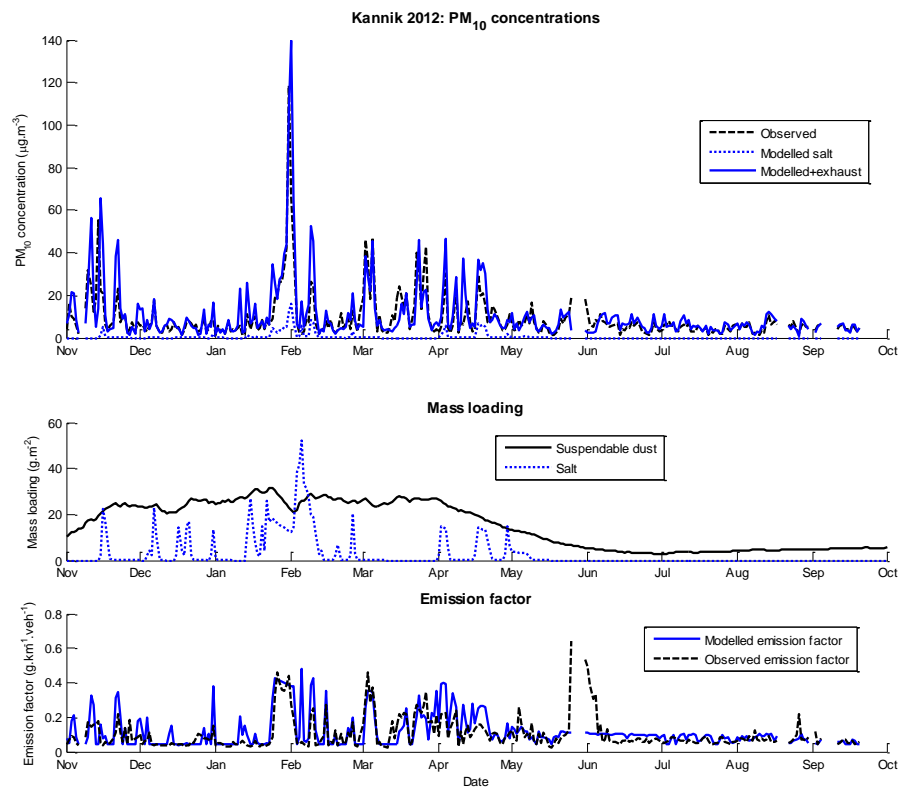


Figure 8: Results of the NORTRIP standalone computations of PM_{10} at Kannik for the period November 2011 to October 2012. Top is the daily mean observed (black dashed) and modelled (blue) concentrations, derived from the emissions using NO_x as a tracer. Middle is the dust (black) and salt (blue) mass loading on the road surface. Bottom is the effective emission factor for both observed (black dashed) and modelled (blue) emissions.

In Figure 9 we summarize the source contributions from the calculated road emissions. Wear sources (road, tire and brake) contribute with 68% of the total modelled PM_{10} concentrations. Exhaust contributes with 26% and road salt contributes with around 4%. Note that road salt is not included in the simplified application of NORTRIP when applied to all road links.

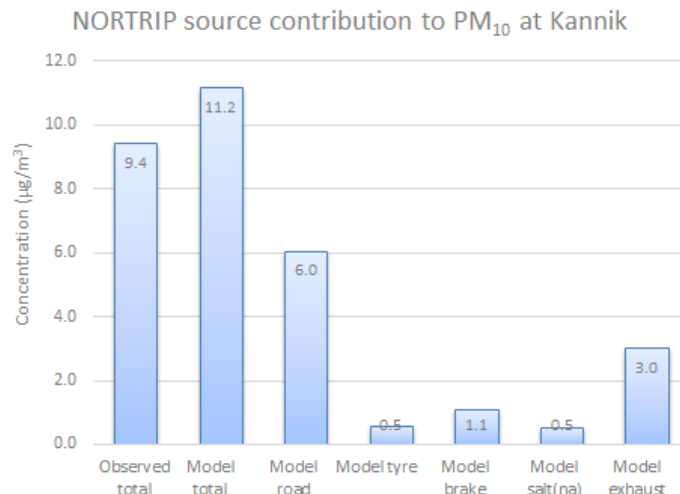


Figure 9: Madlaveien traffic source contributions to PM₁₀ concentrations at Kannik for the period November 2011 to October 2012 using the standalone NORTRIP model.

2.5.2 Application of the NORTRIP model to all roads for mapping

The model is also applied for all 17 888 road links in the modelling region and calculates for each of these the surface dust loading and the dust emissions, but does not calculate emissions due to salt. The emission model is started in November of 2011 in order to build up the road dust depot. Road wear characteristics are dependent on road type with highways having the lowest pavement wear rates and communal roads having the highest.

When applying the model in this way NORTRIP does not calculate the surface moisture separately for each road but calculates the surface moisture for a typically heavily trafficked road (with salting) and a light trafficked road (without salting). The two different surface moistures are then combined with different weightings dependent on road types. Application of the model this way is required because of the time restraints in running the complete moisture model. One drawback when using this method is that vehicle spray is not included as a dust removal process, though drainage is included. This can lead to overestimates of road dust emissions on high speed roads such as highways where removal by water spray may be an important process.

When using the model in this way it is assumed that tunnels are always dry and that only 50% of the emissions within the tunnel emerge at the exists due to deposition within the tunnel.

In Figure 10 the average mass loading, the calculated surface wetness and the total emissions for all roads in the model domain are shown for the year 2012, starting January 1. The first two months of calculations, November and December 2011, are not shown in this case but the road dust depot has already built up by January. Maximum emissions occur out to day 100 (mid-April) and then start to reduce, mainly due to suspension but also due to drainage, after the studded tire season finishes. For the surface wetness the two different modelled road types are show, in green the heavily trafficked road and in pink the light trafficked road. The

impact of traffic on the surface moisture can be seen at around day 25 (end of January) where the heavy trafficked road has dried up but the light trafficked road has not. This period is exactly the period when the highest concentrations of PM₁₀ are both observed and modelled.

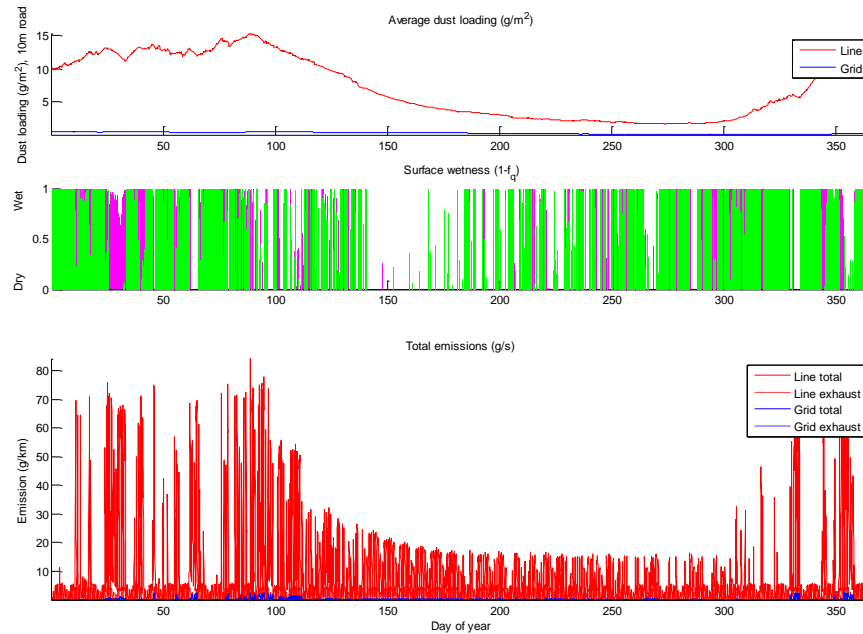


Figure 10: Simplified NORTRIP calculations for all roads in the model domain. Top is the average mass loading for resolved line sources (road links with ADT > 1000 veh/day) in red and for gridded road links (with ADT < 1000 veh/day) in blue. Middle is the surface wetness retention factor showing the heavily trafficked roads (green) and the light trafficked roads (pink) calculations. Bottom is the total emissions from resolved line sources (red) and from gridded line sources (blue) in units of g/s.

In Figure 11 we provide an example of a road dust calculations for the same two roads, Madlaveien and E39, as previously described. These plots cover the entire emission calculation period from November 2011 to December 2012 and are shown in terms of hours since the start of the calculation. Unlike exhaust emissions the road dust emissions are linearly dependent on speed. As a result E39 has significantly higher emissions of PM₁₀ compared to Madlaveien, due to the higher speed limit there.

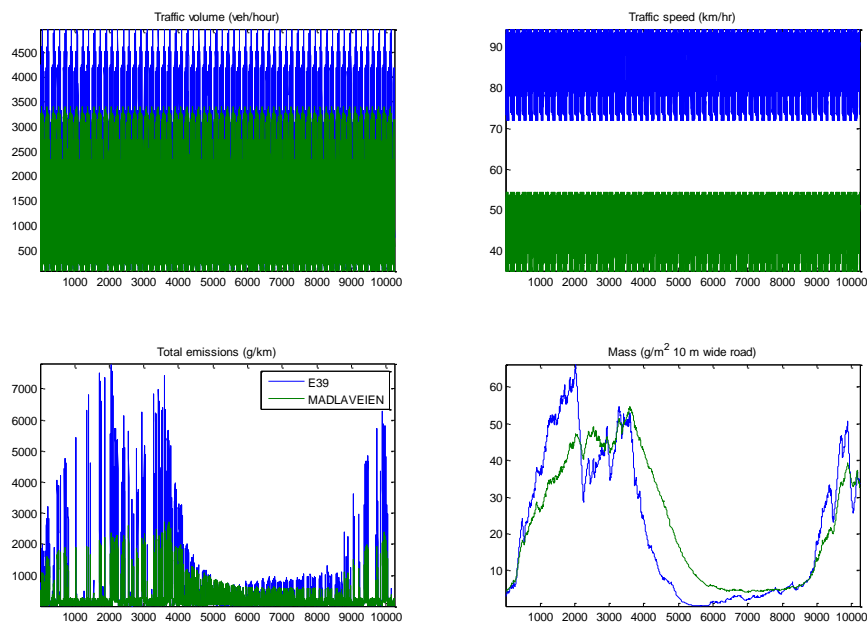


Figure 11: Similar plot to Figure 7 except for total traffic related PM_{10} emissions. The bottom right plot shows the mass loading on the two roads. The period covered is from 1 November 2011 to 31 December 2012

3 Modelling

The air quality model used is the EPISODE model, developed at the Norwegian Institute for Air Research (NILU, www.nilu.no). This model has been used for a large number of applications and is part of the Bedre Byluft forecasting system for Nord-Jæren and five other city regions in Norway (www.luftkvalitet.info). The model calculates the dispersion and transport of pollutants as well as the chemical reaction of NO with ozone to produce NO_2 .

The EPISODE model uses two separate models to calculate concentrations. The first is a so called ‘gridded model’ which calculates the urban background concentrations. This model uses a grid of $1 \times 1 \text{ km}^2$ and calculates emissions, meteorology and concentrations in this grid region, which is 14 km in the East-West direction and 25 km in the North-South direction. The model contains 13 vertical layers, with the lowest at 10 m. These layers increase in thickness with height. This model cannot resolve the high concentrations close to roads and so an additional ‘line source model’ is used to calculate concentrations near roads. The line source model calculates concentrations not in a grid but at particular points in space, known as receptor points. This allows the model to calculate concentrations at exactly the position of the monitoring station and to resolve the steep gradients in concentration as you move away from the road source.

The EPISODE model combines these two types of models to calculate concentrations throughout the Nord-Jæren region. In this case gridded maps at 100 m resolution are made. Each of these grid values represents the average concentrations in a $100 \times 100 \text{ m}^2$ area. To achieve this a large number of receptor

points are placed in the region (33 000), with the highest number of points being placed close to roads. Near road receptor points are placed approximately 20 m from the centre of the road. All these receptor points are then used to calculate the average concentration in the 100 x 100 m² grids (Section 7.1).

The model does not include the effect of buildings so the results represent the concentrations if buildings were not in place. In some inner city areas where tall buildings can block or redirect the flow of air, then the model will not provide ideal results. However, in areas where buildings are one or two stories high then the model is more representative.

In order for the model to calculate both the dispersion and the transport of pollutants then meteorological data concerning wind speed and direction, as well as atmospheric stability, is required. To this end observations from the airport in Sola, from a meteorological station in Stavanger-Våland and from a meteorological station in Særheim are used (Section 3.1). The observed winds are interpolated from these measurements and are adjusted for topography and surface conditions, e.g. land or sea, built up or open. The resulting wind field is then an approximation of the wind field over the entire region.

In addition to the local contribution of emissions to air quality in Nord-Jæren the air blowing into this region is also polluted to some extent. It is thus necessary to determine what this level of pollution is. For ozone we use a regional background measurement station in Sandve, 40 km North-West of Stavanger. Unfortunately measurements of NO₂ and PM₁₀ are not available in this region and so the regional background contribution is estimated using the minimum measured hourly concentration over the last 24 hours (Section 3.2).

The air quality model has a number of uncertainties and for this reason it is necessary to compare the results with measured pollutants (Section 5). Model uncertainties include the uncertainties in the meteorological wind fields as well as the impact of buildings and other structures on the wind fields near roads. For example, exactly how the wind varies near the Kannik station is not exactly known. Though the road is to some extent open, there is always some degree of channelling of the wind along roads and the strength of the wind can also be affected by local conditions such as buildings.

3.1 Meteorological data and modelling

Meteorological fields are determined using observed meteorology combined with the mass conserving wind field interpolation model MCWIND. Prognostic meteorological fields, as produced for the Bedre Byluft forecasts in Nord-Jæren, were not available for the entire assessment period (winter only) and so these were not used for the air quality modelling here.

The meteorological data comes from the airport at Sola, from a meteorological station in Særheim, close to the southern border of the model grid, and a station at Stavanger-Våland. The available meteorological data required by the model for the year 2012 is listed in Table 3. As can be seen, there is no single station that provides all the necessary data.

Table 3. Overview of available meteorological data for the wind field and NORTRIP modelling. *Red* indicates these data were used in the modelling. 'All' indicates that the entire year 2012 is available.

Station	Sola	Særheim	Stavanger-Våland
Wind speed	All	All	
Wind direction	All	All	
Temperature	All	All	All
Relative humidity			All
Precipitation		All	All
Global radiation		Missing 22.05-03.07. Use 2011 data	
Cloud cover	All		
Position (lat, lon)	58.8843 5.637	58.7605 5.6505	58.9572 5.73

A time series of relevant meteorological parameters used in the model are shown in Figure 12. As can be seen both the wind speed and the wind direction are very similar at both the Sola and Særheim sites, despite the distance between the two stations being approximately 15 km. It is unfortunate that there is no wind data available from the Stavanger-Våland station as this could have provided extra meteorological information in the most important modelling area.

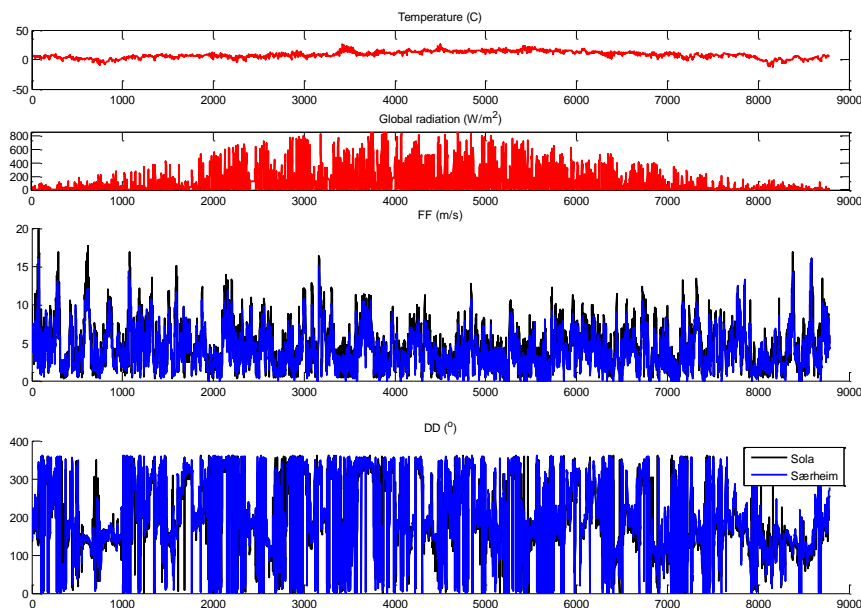


Figure 12: Hourly meteorological data used in the calculations. Wind speed and direction are available from both Sola and Særheim stations. Temperature is taken from Stavanger-Våland and global radiation from Særheim.

Meteorological input data is provided to MCWIND, the mass conserving wind model used at NILU for interpolating wind fields to the model grid. Interpolation of the wind is carried out using surface roughness data and topography data available through the Bedre Byluft project.

3.2 Regional background concentrations

Except for ozone, regional background concentrations are not available close to Nord-Jæren. Because of this, background contributions are estimated by taking the minimum concentration within a 24 hour moving window from the two available observation stations at Kannik and Våland for NO_x , NO_2 and PM_{10} . Other possible sources of regional background data include the measurements at Birkenes, 200 km away, and from regional scale chemical transport models. Annual mean concentrations have been assessed using MACC-2 modelling data (MACC, 2013). Examples of MACC-2 model concentrations in the Nord-Jæren region are shown in Figure 13. In Table 4 we compare the annual mean concentrations based on these three sources. The background levels derived from MACC-2 modelling data are given a range as there are significant gradients in the data due to sea salt for PM_{10} and due to shipping for NO_2 .

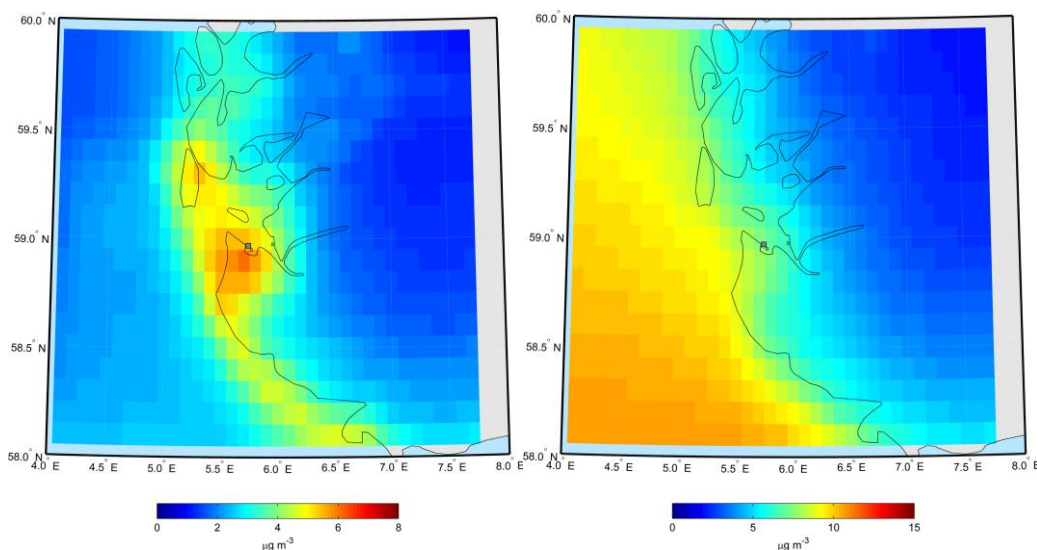


Figure 13: Annual mean concentrations for NO_2 (left) and PM_{10} (right) for 2012 derived from the MACC-2 model ensemble calculations in the Nord-Jæren region.

Table 4: Estimates of annual mean background concentrations using three different sources of information. See text for details.

Method/source	NO_x ($\mu\text{g}/\text{m}^3$)	NO_2 ($\mu\text{g}/\text{m}^3$)	PM_{10} ($\mu\text{g}/\text{m}^3$)	$\text{PM}_{2.5}$ ($\mu\text{g}/\text{m}^3$)
24 hour minimum from local stations	11.1	7.6	7.2	3.6
Birkenes	NA	3.4	5.3	3.4
MACC-2 modelling	NA	5 - 6	6 - 8	NA

There is clearly some uncertainty in the regional background concentrations in the calculations. For all compounds this uncertainty is approximately $\pm 2 \mu\text{g}/\text{m}^3$.

3.3 NO₂ chemistry parameterisation

In this current application an additional parameterisation for the NO₂ chemistry has been implemented to better describe the reaction rate for the conversion of NO to NO₂ with ozone close to source. In the standard EPISODE NO₂ calculations the photo-stationary assumption is applied, which assumes that a balance is achieved between the conversion of NO to NO₂ through O₃ and the photo-disassociation of NO₂ to NO through UV sunlight. Reaction rates for the NO to NO₂ conversion are just a couple of minutes and for the photo-disassociation this occurs on time scales of up to an hour. This means that for the gridded concentrations the photo-stationary assumption is appropriate but for sources close to roads this is not the case, as it takes several minutes for the fastest reaction to be completed.

To improve this within the EPISODE modelling structure a routine has been introduced that limits the available NO for the chemical reaction, based on the travel time from the road source, in the line source model. This is achieved by determining the time scale of the reaction, derived from the reaction rate and the ozone concentrations, and calculating the downwind travel time from the road link to the receptor point. Exponential damping of the available NO for the photo-stationary calculation, based on this time scale, is then applied. For receptors very close to roads there will be little NO available for the reaction, for receptors further from the road source (or during weak wind situations) more NO will be available.

The methodology was applied and tested at the Kannik station site where it was found to improve both the correlation and the NO₂/NO_x ratio calculated there. The major spatial impact of this parameterisation is to reduce the gradient in NO₂ concentrations with distance from the road. Thus PM₁₀ or NO_x concentration gradients will be steeper as you move away from the road compared to NO₂ gradients.

The formulation is summarised as follows:

The reaction rate (R_1) and the reaction time scale (τ_1) are determined from the ozone concentrations ($[O_3]$) in mol/cm³ and atmospheric temperature in Kelvin (T_{air})

$$R_1 = 1.4 \times 10^{-12} \exp\left(\frac{-1310}{T_{air}}\right)$$

$$\tau_1 = \frac{1}{R_1 [O_3]}$$

The reaction time (t) of the air from the road to the receptor is given by

$$t = \frac{D}{U} + t_0$$

Where U is the wind speed, D the upwind distance to the road from the receptor and τ_0 is an initial mixing time scale. The damping of NO concentrations is then given by the factor s_{NO} as

$$s_{NO} = 1 - \exp\left(\frac{-t}{\tau_1}\right)$$

4 Analysis of measurements

A short analysis of the measurements was carried out to ascertain if there were any bias or inconsistencies in the data. The data used was downloaded from the 'luftkvalitet.info' administrative site and only approved data, quality controlled by NILU in their role as reference laboratory, was used. Data available is from the traffic site Kannik and the urban background site Våland. The positions of the stations are shown in Figure 14.

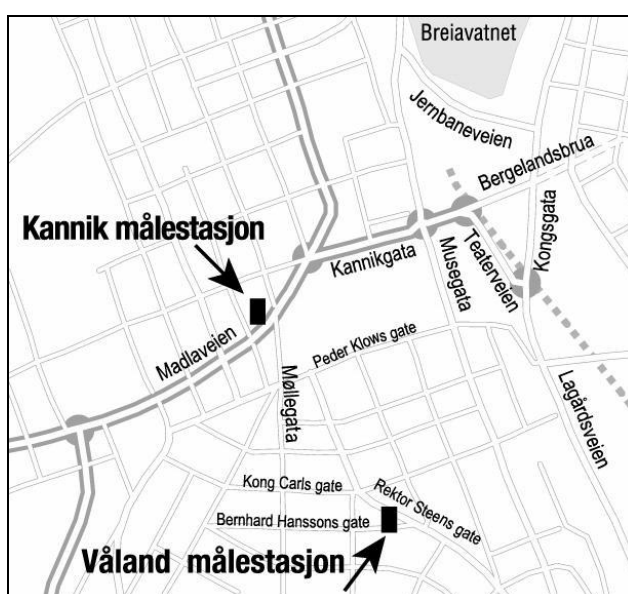


Figure 14: Position of the measurement stations in Stavanger. Taken from 'Luftkvalitet Stavanger, årsrapport 2012' (Stavanger kommune, 2013).

4.1 Offset in NO₂ and NO_x measurements

To assess any possible bias in the measurements the lowest 500 ranked concentrations were plotted in ranked order. It is expected that the lowest values should approach 0 if there are no systematic offset of the data. The results for NO₂ and NO_x, at both stations, are shown in Figure 15. The figures indicate a possible offset of around 6 µg/m³ for NO₂ and 10 µg/m³ for NO_x at the Kannik station but no significant offset at Våland. If this offset is consistent throughout the measurement period then this implies that the measured concentrations for NO₂ are 6 µg/m³ higher than they should be. This analysis cannot categorically state that the measurements at Kannik are too high but they do indicate the possible uncertainty in the observations. No significant systematic offset was seen in the PM measurements.

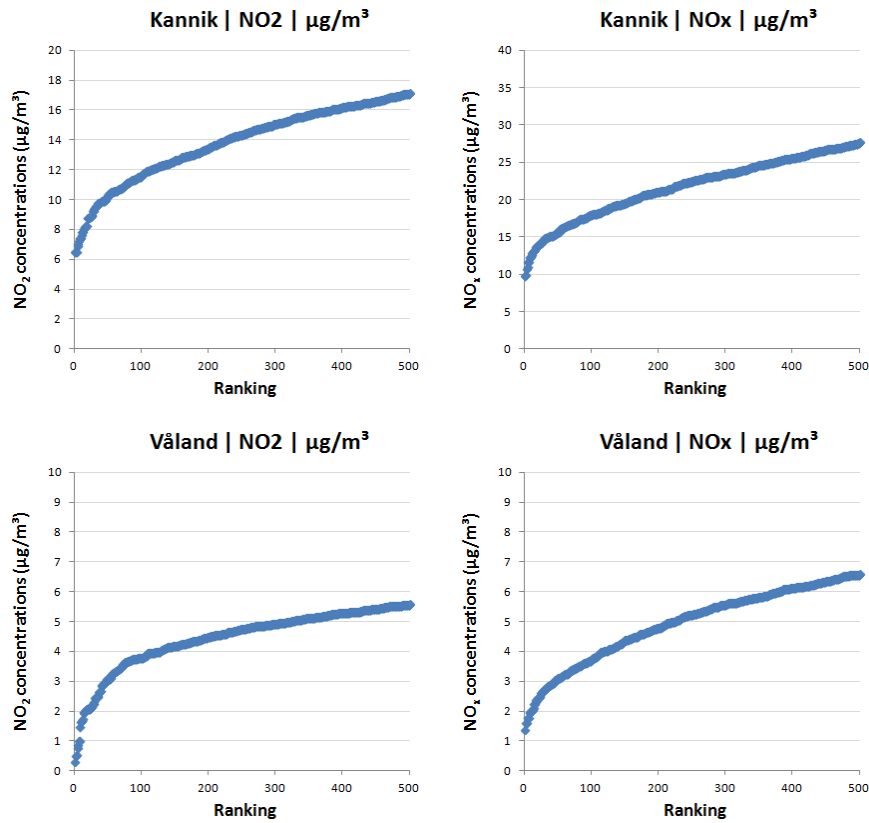


Figure 15: Lowest ranked 500 hourly mean measurements of NO_2 and NO_x at Kannik (top) and Våland (bottom) stations.

4.2 Ratio of NO_2 and NO_x

In addition to the ranking, hourly mean NO_2 was plotted against NO_x . This was principally to look for inconsistencies in the data but also to determine the limits of the NO_2/NO_x ratio as this indicates whether the emission ratios used in the traffic emission factors are realistic or not. For the traffic station Kannik, the lower limit slope, represented by the minimum ratio of NO_2/NO_x for higher NO_x concentrations, is seen in Figure 16 to be from 11% to 16%. This minimum ratio will occur under high concentrations and/or low ozone levels and is indicative of the actual emission ratio from the traffic emissions, when little NO is converted to NO_2 . The calculated emission ratio for Madlaveien in the model, with 8% HDV, is 13.5% under congested conditions which agrees with the observed ratio. The average observed ratios of NO_2/NO_x at the two stations Kannik and Våland are 40% and 65% respectively

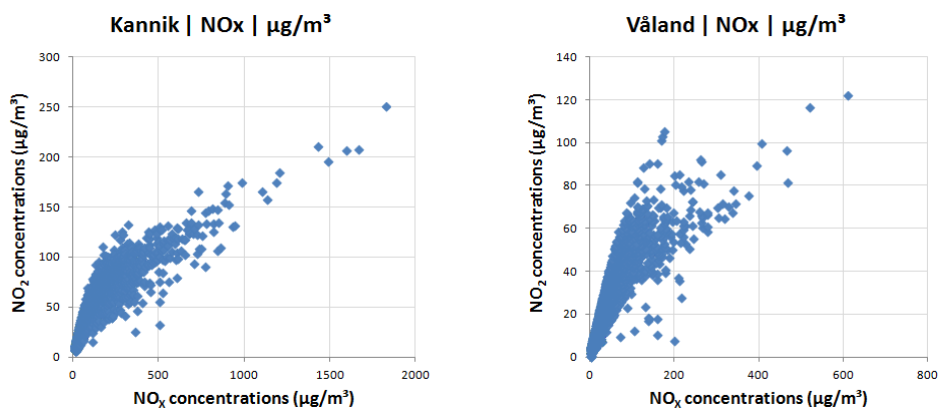


Figure 16: Hourly mean NO_2 versus NO_x concentrations for Kannik and Våland.

4.3 Ratio of $PM_{2.5}$ and PM_{10}

As previously mentioned no systematic offset was seen for the PM measurements. Plots of $PM_{2.5}$ against PM_{10} were made to check for consistency between $PM_{2.5}$ and PM_{10} . These plots are shown in Figure 17. It is expected that the upper limit slope of the scatter is the 1:1 line as this represents the situation where all PM_{10} is in $PM_{2.5}$. The lower limit of the scatter would represent the situation where the PM concentrations have their most ‘course’ origin, likely during road dust dominating periods. This should be most obvious at the traffic station Kannik.

From the plots we find an upper limit slope ($PM_{2.5}/PM_{10}$) of around 0.7 - 0.8 for both stations and a lower limit slope of 0.05 for Kannik and 0.1 – 0.2 for Våland. The upper limit slope does not reach unity partially because a correction factor of 1.1 is applied to PM_{10} concentrations but not to $PM_{2.5}$. Even so the slope is still slightly less than unity. It is expected that the higher $PM_{2.5}$ concentrations are during wood burning episodes and these results indicate that the ratio of $PM_{2.5}/PM_{10}$ in these emissions is more likely to be 0.8 – 0.9. Currently the model assumes all wood burning emissions to be $PM_{2.5}$. The lower limit slope for Kannik agrees with previous observations in other Nordic countries (Denby and Sundvor, 2012) that indicate that from 3 – 7 % of PM_{10} from road dust emissions is in $PM_{2.5}$. The NORTRIP models uses a value of 5% when calculating $PM_{2.5}$ emissions.

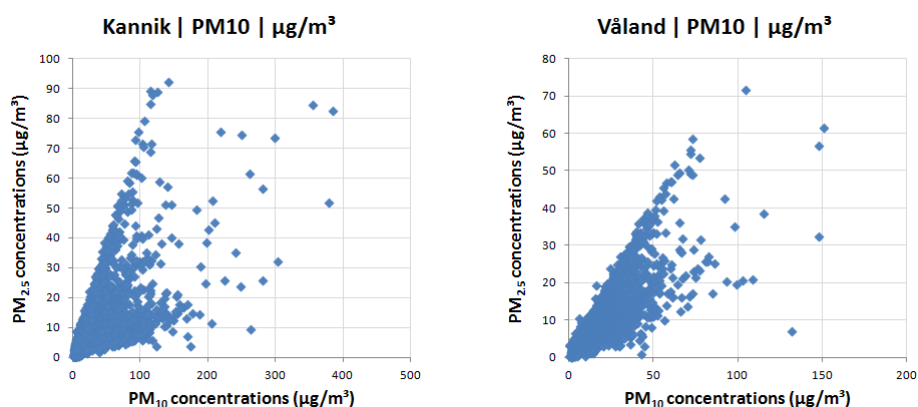


Figure 17: Hourly mean $PM_{2.5}$ versus PM_{10} concentrations for Kannik and Våland.

5 Validation

Model calculations are compared with observed concentrations at the measurement sites of Kannik and Våland. The comparison consists of a visual representation of the results in terms of time series data and also as a statistical analysis.

5.1 NO₂

In Figure 18 we show daily mean NO₂ concentrations at both stations over the entire year and in Figure 19 the average daily cycle. Daily mean variation is fairly well represented by the model. The average daily cycle is not as well represented by the model at Kannik. This daily cycle will be strongly regulated by the daily traffic cycle which is not known for this road. The daily traffic cycle used is probably not representative for this site.

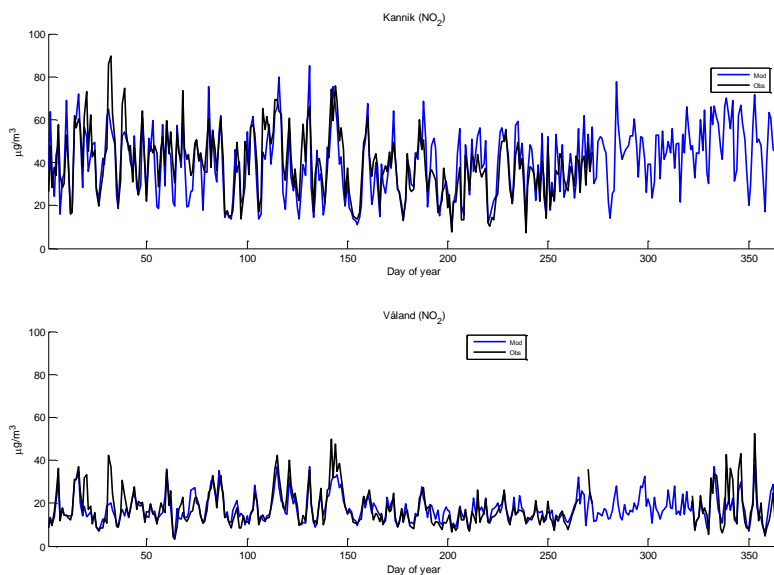


Figure 18: Daily mean concentration of NO₂ at the two measurement stations Kannik and Våland. Blue is modelled and black is observed.

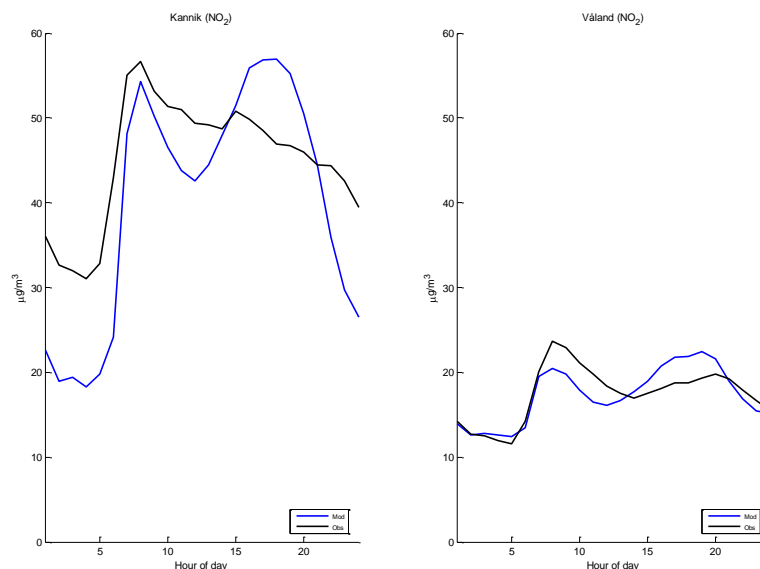


Figure 19: Average daily cycle of NO_2 concentrations at the two measurement stations Kannik and Våland. Blue is modelled and black is observed.

In Table 5 we show the statistical analysis of hourly mean concentrations for NO_2 at both stations. At Kannik the annual mean is underestimated by approximately 15% but the 19th highest hourly mean is slightly overestimated. Hourly mean correlation is quite high at this site with $R^2 = 0.41$, meaning that 41% of the hourly variability is explained by the model. At Våland the model represents very well the annual mean and 19th highest hourly mean concentrations. Correlation is lower with $R^2 = 0.29$. There is very little contribution from the line source model at this site and so these concentrations are representative of the urban background levels.

Table 5: Statistical assessment of the hourly model performance for NO_2 compared to measurements

Parameter	Kannik	Våland
Observed mean ($\mu\text{g}/\text{m}^3$)	45.0	17.5
Modelled mean ($\mu\text{g}/\text{m}^3$)	37.8	17.1
Observed 19th highest hourly mean ($\mu\text{g}/\text{m}^3$)	127.7	82.3
Modelled 19th highest hourly mean ($\mu\text{g}/\text{m}^3$)	142.3	81.8
Observed exceedances of hourly limit value	1	0
Modelled exceedances of hourly limit value	0	0
Correlation (R^2)	0.41	0.29
Observational coverage (%)	74	85

5.2 O_3

In Figure 20 we show daily mean observed ozone (O_3) concentrations from the regional background station Sandve plotted together with the model calculated O_3 at both stations over the entire year. In Figure 21 the average daily cycle is also shown. The daily mean time series shows the measured regional background concentrations compared to the modelled concentrations at the measurement sites. Ozone levels are always lower at the measurement sites due to the chemical

reaction with the emissions of NO. Ozone levels are lowest at the Kannik site. The daily cycle plot shows that the regional background levels of ozone have a distinct daily cycle and are highest in the early afternoon. The difference between the modelled and regional background ozone concentrations show how much ozone is used to create NO₂ from NO. This conversion peaks during the highest emission periods.

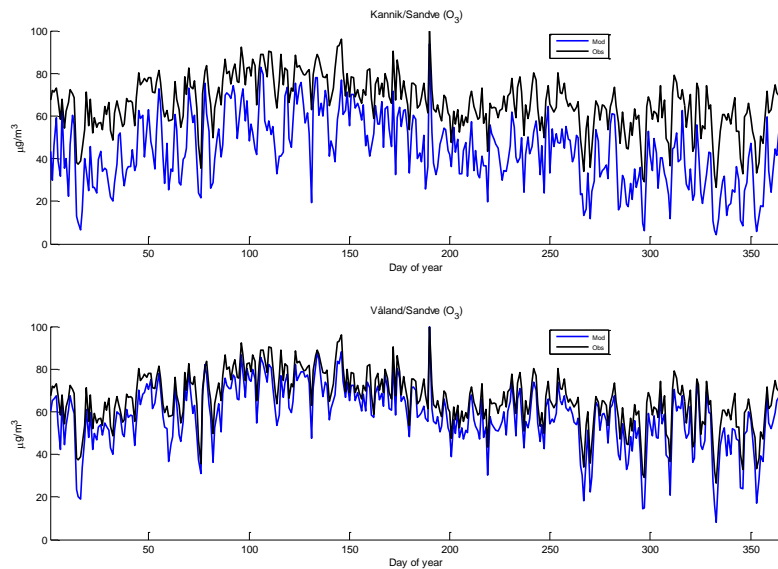


Figure 20: Daily mean concentration of modelled O₃ concentrations at the two measurement stations Kannik and Våland (blue). Also included are the concentrations from the regional background site at Sandve (black).

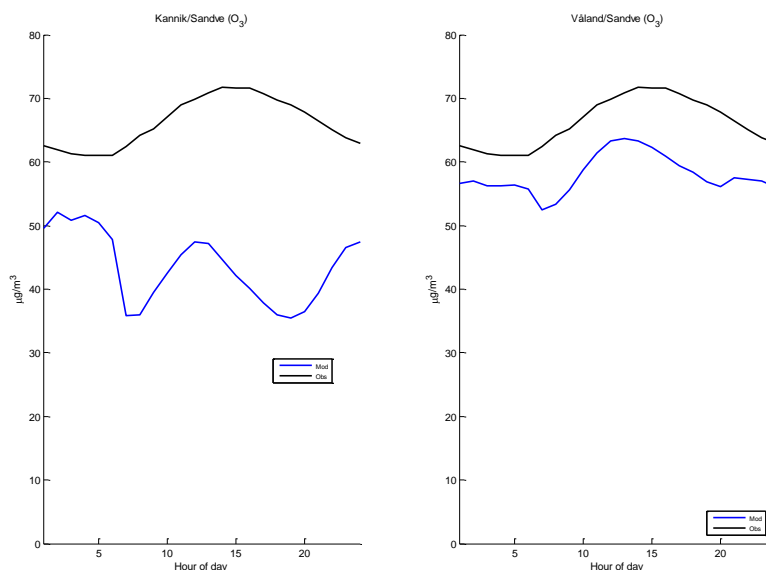


Figure 21: Average daily cycle of modelled O₃ concentrations at the two measurement stations Kannik and Våland (blue). Also included are the concentrations from the regional background site at Sandve (black).

5.3 NO_x

In Figure 22 we show daily mean NO_x concentrations at both stations over the entire year and in Figure 23 the average daily cycle. The daily mean time series is fairly well represented by the model, similar to NO₂, but with greater variability. The average daily cycle at Kannik is slightly different for NO_x than NO₂. NO_x shows a lower peak in the afternoon as there is generally more ozone available in the afternoon for the creation of NO₂. This daily cycle will be strongly regulated by the daily traffic cycle which is not known for this road.

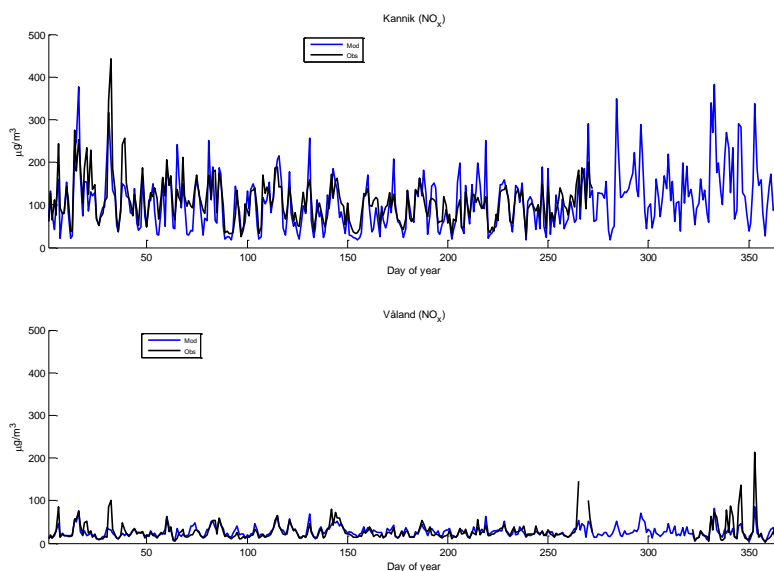


Figure 22: Daily mean concentration of NO_x at the two measurement stations Kannik and Våland. Blue is modelled and black is observed.

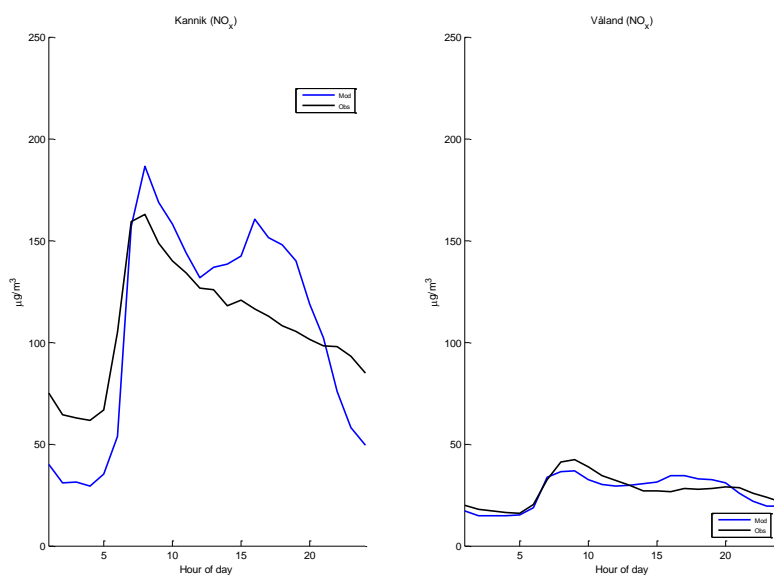


Figure 23: Average daily cycle of NO_x concentrations at the two measurement stations Kannik and Våland. Blue is modelled and black is observed.

In Table 6 we show the statistical analysis of hourly mean concentrations for NO_x at both stations. In this case there are no limit values and so the 90'th percentile is shown instead to indicate the model prediction of higher percentiles. At Kannik the annual mean is underestimated by approximately 10% but the 19'th highest hourly mean and 90'th percentile are overestimated. Correlation is lower than for NO_2 with $R^2 = 0.32$. The inclusion of observed ozone in the model, which leads to the creation of NO_2 , often increases the correlation of the model. At Våland the model represents very well the annual mean and 90'th percentile but over estimates the 19'th highest hourly mean concentrations. Correlation is lower with $R^2 = 0.18$.

Table 6: Statistical assessment of the hourly model performance for NO_x compared to measurements

Parameter	Kannik	Våland
Observed mean ($\mu\text{g}/\text{m}^3$)	107.7	27.1
Modelled mean ($\mu\text{g}/\text{m}^3$)	97.4	26.2
Observed 90'th hourly mean percentile ($\mu\text{g}/\text{m}^3$)	202.4	50.1
Modelled 90'th hourly mean percentile ($\mu\text{g}/\text{m}^3$)	218.4	47.3
Observed 19th highest hourly mean ($\mu\text{g}/\text{m}^3$)	644.8	277.6
Modelled 19th highest hourly mean ($\mu\text{g}/\text{m}^3$)	845.8	197.6
Correlation (R^2)	0.32	0.18
Observational coverage (%)	74	85

5.4 PM_{10}

In Figure 24 we show daily mean PM_{10} concentrations at both stations over the entire year and in Figure 25 the average daily cycle. Daily mean variation is well represented by the model at Kannik, which is strongly influenced in the winter and spring by road dust emissions. The model tends to underestimate concentrations over the entire year at both stations. The average daily cycle is fairly represented by the model at both sites but underestimates concentrations.

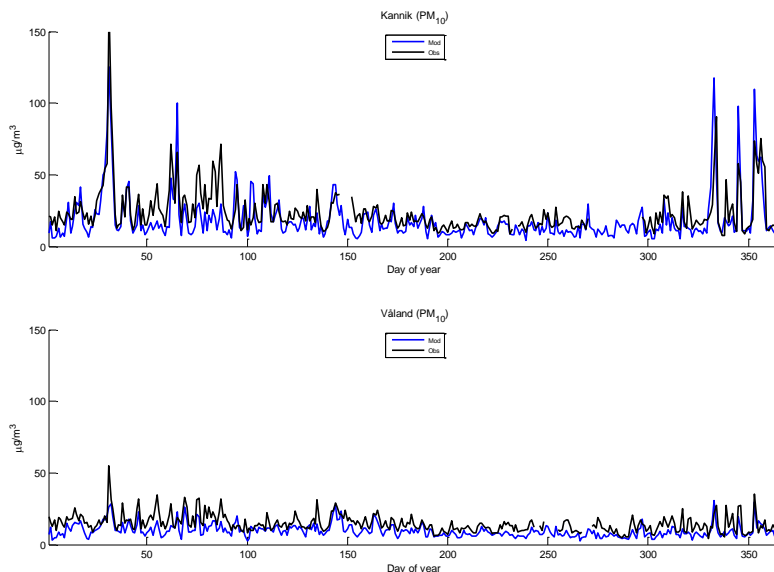


Figure 24: Daily mean concentration of PM_{10} at the two measurement stations Kannik and Våland. Blue is modelled and black is observed.

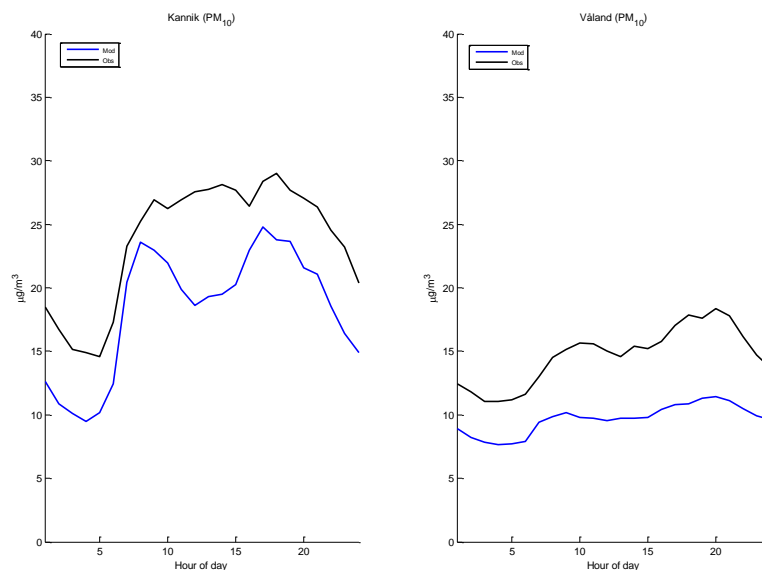


Figure 25: Average daily cycle of PM_{10} concentrations at the two measurement stations Kannik and Våland. Blue is modelled and black is observed.

In Table 7 we show the statistical analysis of hourly mean concentrations for PM_{10} at both stations. At both sites the annual mean is underestimated by approximately $5 \mu\text{g}/\text{m}^3$ and the 36th highest daily mean is also underestimated by approximately $7 \mu\text{g}/\text{m}^3$. Despite this, correlation is quite high at both sites with $R^2 = 0.59$ and 0.49 at Kannik and Våland respectively. The underestimation is likely due to missing emissions, either non-anthropological sources such as sea salt or due to an underestimate of existing sources, such as domestic wood burning. It may also be the result of an under estimate of the regional background

contribution, which are based on the local 24 hour minimum concentrations. The underestimation is visible throughout the year.

Table 7: Statistical assessment of the hourly model performance for PM_{10} compared to measurements

Parameter	Kannik	Våland
Observed mean ($\mu\text{g}/\text{m}^3$)	23.7	14.6
Modelled mean ($\mu\text{g}/\text{m}^3$)	18.9	9.7
Observed 36 th highest daily mean ($\mu\text{g}/\text{m}^3$)	39.18	22.9
Modelled 36 th highest daily mean ($\mu\text{g}/\text{m}^3$)	32.1	15.7
Observed exceedances of daily limit value	22	1
Modelled exceedances of daily limit value	14	0
Correlation (R^2)	0.59	0.49
Observational coverage (%)	89	95

5.5 $PM_{2.5}$

Due to the relevance of $PM_{2.5}$ to PM_{10} , model calculations were also carried out for $PM_{2.5}$, though no maps of this compound were made. In Figure 26 we show daily mean $PM_{2.5}$ concentrations at both stations over the entire year and in Figure 27 the average daily cycle. The daily mean time series is fairly well represented by the model at Kannik, though the model appears to overestimate the concentrations in the spring period. The average daily cycle is similar to that for PM_{10} . The wood burning peak can be clearly seen at around 21:00 in both model and observation, particularly at Våland.

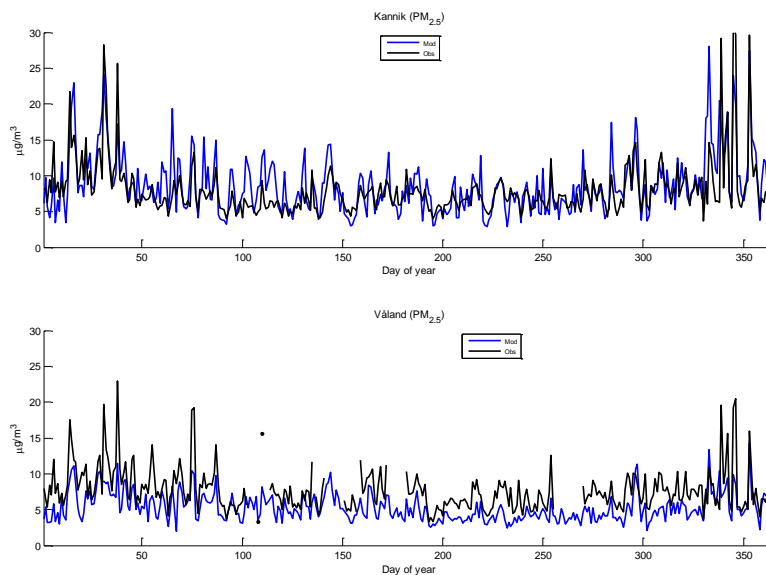


Figure 26: Daily mean concentration of $PM_{2.5}$ at the two measurement stations Kannik and Våland. Blue is modelled and black is observed.

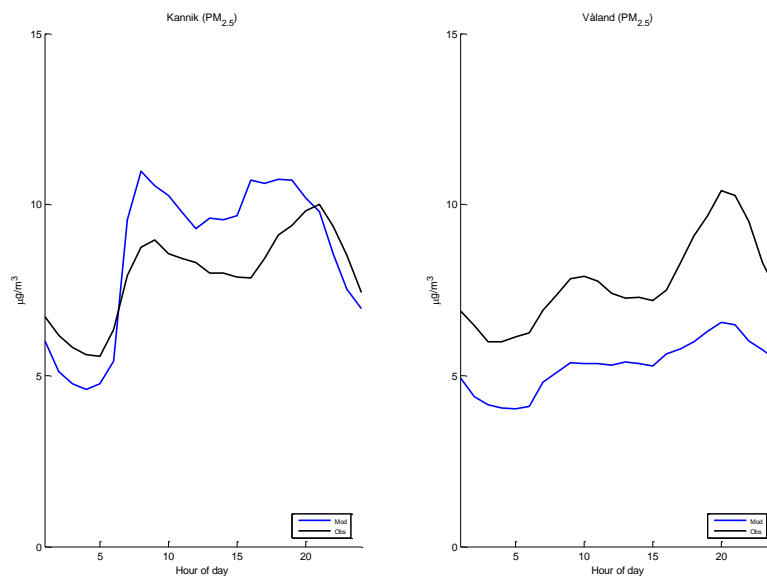


Figure 27: Average daily cycle of $PM_{2.5}$ concentrations at the two measurement stations Kannik and Våland. Blue is modelled and black is observed.

In Table 8 we show the statistical analysis of daily mean concentrations for $PM_{2.5}$ at both stations. Since there are no daily mean limit values associated with $PM_{2.5}$ we show the 90'th percentiles. Unlike PM_{10} , which shows a significant difference in concentrations between the two sites, the observed average $PM_{2.5}$ concentrations are very similar at both measurement sites despite the stronger influence of traffic at Kannik. This is to some extent counter intuitive and may indicate measurement error at one, or both, of the stations. We find that the model overestimates the $PM_{2.5}$ concentrations at Kannik slightly. At Våland the annual mean is underestimated by $2.4 \mu\text{g}/\text{m}^3$. More than half of the modelled $PM_{2.5}$ concentrations come from the regional background contribution ($3.6 \mu\text{g}/\text{m}^3$). Correlation is only slightly lower than for PM_{10} .

Table 8: Statistical assessment of the hourly model performance for $PM_{2.5}$ compared to measurements.

Parameter	Kannik	Våland
Observed mean ($\mu\text{g}/\text{m}^3$)	8.0	7.7
Modelled mean ($\mu\text{g}/\text{m}^3$)	8.6	5.3
Observed 90'th daily mean percentile ($\mu\text{g}/\text{m}^3$)	11.4	10.9
Modelled 90'th daily mean percentile ($\mu\text{g}/\text{m}^3$)	13.6	7.9
Correlation (R^2)	0.51	0.48
Observational coverage (%)	99	86

6 Modelled source apportionment

Source apportionment at the monitoring sites is carried out using the model. The model is run for a number of different sources and the concentrations for NO_x and PM₁₀ are determined per source. An overview of the calculated source contributions is given in Table 9.

These results indicate clearly the dominance of the traffic exhaust for the NO_x concentrations at the Kannik station. The contribution from traffic is significantly less at Våland and is similar to the contribution from the regional background. For PM₁₀ the dominant contributor at Kannik is traffic, both non-exhaust and exhaust, but the regional background also contributes significantly. At Våland the traffic contribution is similar to the home heating but the largest contribution is from the regional background.

Table 9: Overview of the source contributions for PM₁₀ and NO_x at the two monitoring sites as calculated by the model.

Source	Kannik PM ₁₀ (µg/m ³)	Våland PM ₁₀ (µg/m ³)	Kannik NO _x (µg/m ³)	Våland NO _x (µg/m ³)
Regional background	7.2	7.1	11.6	10.6
Heating	1.1	1.0	0.22	0.25
Other area	0.09	0.07	0.76	0.65
Shipping (and rail)	0.06	0.03	5.6	2.6
Traffic exhaust	3.0	0.46	81.0	13.6
Traffic non-exhaust	7.5	1.17	0	0
Mean modelled	19.1	9.8	99.1	27.7
Mean observed	23.8	14.7	107.7	27.1
Missing	4.7	4.8	8.6	-0.5

6.1 NO_x source contribution and temporal variability

The weekly mean NO_x concentrations, presented per source, are shown in Figure 28. These show the dominance in traffic exhaust emissions at Kannik. Contributions are highest during the winter period due to the more stable atmospheric conditions. For Våland the contributions are fairly homogenous over the entire year with highest background concentrations in the summer.

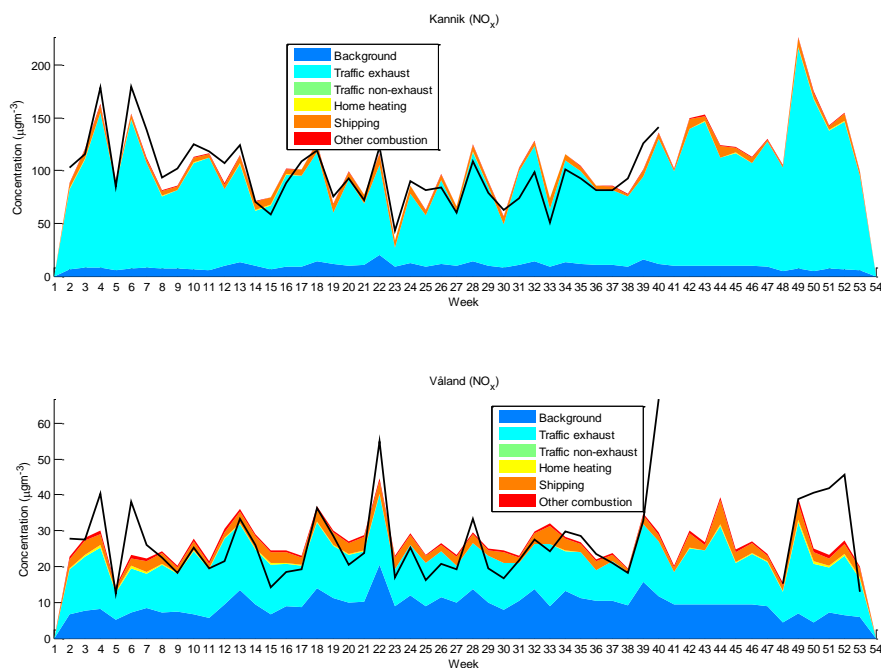


Figure 28: Weekly mean modelled source contributions at the two measurement sites Kannik (top) and Våland (bottom) for NO_x . Observed total concentrations are shown as a black line. The vertical scales are different for the two sites.

6.2 PM_{10} source contribution and temporal variability

The weekly mean PM_{10} concentrations, presented per source, are shown in Figure 29. These show the dominance of traffic non-exhaust emissions at Kannik during the winter and spring but also indicates that these non-exhaust emissions persist throughout the year. At Våland the entire year is dominated by the regional background contribution

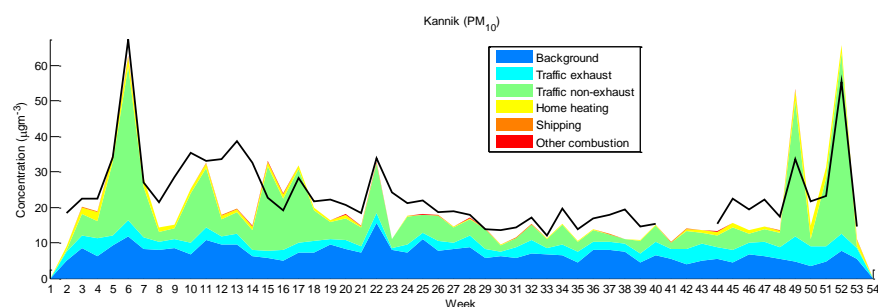


Figure 29: Weekly mean modelled source contributions at the two measurement sites Kannik (top) and Våland (bottom) for PM_{10} . Observed total concentrations are shown as a black line. The vertical scales are different for the two sites.

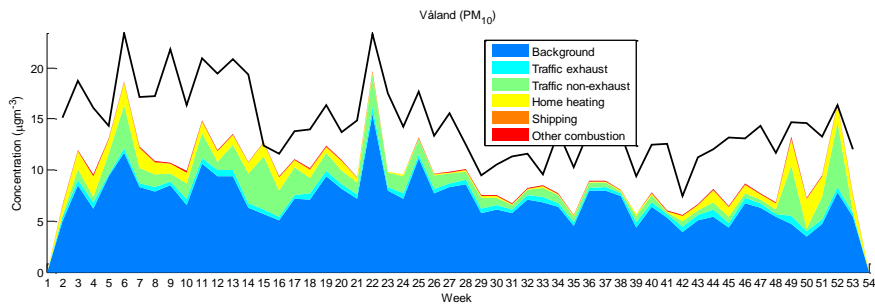


Figure 29: Contd.

7 Mapping method and maps

In the previous sections concentrations have been presented at the measurement sites only. In order to make maps of air quality, concentrations must be modelled throughout the model domain. Maps of NO₂ annual mean, NO₂ 19th highest hourly mean, PM₁₀ annual mean and PM₁₀ 36th highest daily mean are to be made at 100 m resolution for the Nord-Jæren region. The choice of using the percentiles, instead of the number of exceedance hours or days, is made because often there are no modelled exceedances and so the percentiles provide a more useful map.

In the following sections the mapping methodology is explained and then the final maps are presented, as they appear in the summary report.

7.1 Mapping receptors and post processing

In order to create maps at 100 m resolution special routines have been developed within the MATLAB programming routines. To achieve the required resolution the model domain is populated with a large number of receptor points (33 000). These receptor points are placed with higher density near roads, out to the extent of the road link influence distance (400 m), the distance to which the line source model is applied. Outside of this region receptor points are placed every 500 m in a regular grid as these sample only from the grid model. The mapping process consists of pre-processing of receptor points and post-processing for creating the maps as follows:

Pre-processing

1. Road links of length > 15 m are selected
2. For each selected road link receptor points are placed on both sides of the road at 75 m intervals and at 15 m, plus half a road width, distance from the road link.
3. This is repeated at distances of 55, 125, 250 and 450 m from the road. For each increasing distance the space between the receptor points, parallel to the road, increase from the initial 75 m to 100, 150, 200 and 300 m. The

distribution takes the receptor points just beyond the line source influence distance of 400 m.

4. A 500 m square grid of regular receptor points is then added to cover the entire model domain in areas where the grid model alone is used to calculate concentrations
5. The position of all the receptor points is then assessed. All receptor points within 20 m of roads are removed so that no receptor points are close than this distance.
6. Receptor points within 25 m of other receptors are also removed as is this the specified maximum resolution.
7. The resulting array of receptor points is shown in Figure 30.

Post-processing

1. The model calculates concentrations at all the mapping receptor points and saves the annual mean concentrations, the number of exceedances above the prescribed limit value and the related percentiles for each limit value. Example receptor point concentrations are shown in Figure 31 top left. The model also saves the same type of concentration data for each model grid.
2. The EPISODE model calculates concentrations at the receptor points by adding line source and grid model concentrations. No interpolation of the gridded concentrations is applied, often leading to clearly visible ‘grid shapes’ in the receptor point concentration data. To obtain smoother variations in the map, related to gridded concentrations, the receptor data is post-processed. The gridded concentration fields are interpolated, using a cubic spline interpolation, at all receptor points. The original gridded concentrations are then subtracted from all receptor points and the interpolated gridded concentrations are added back. This creates a smooth concentration surface for the grid model contribution but does not change the line source contribution. Example smoothed grid receptor point concentrations are shown in Figure 31 top right.
3. The new receptor point data is then linearly interpolated to a 20 m sub-grid throughout the entire model domain creating a high resolution map. Example 20 m grid concentrations are shown in Figure 31 bottom left.
4. This interpolated sub-grid is then aggregated into 100 m grids by taking the mean of the sub-grids. Maximum sub-grid values are also calculated for each 100 m grid but are not used in the maps. In this way the 20m sub-grid interpolation is used as a numerical integration method to determine the means in the 100 m mapping grids.
5. The two outmost 100 m grids are subject to interpolation errors and these are removed from the final maps. Example 100 m grid concentrations are shown in Figure 31 bottom right. (NOTE: Since creating these files the interpolation method has been updated. By placing outer edge gridded 1 km concentrations just outside the edge of the domain, before interpolating to the 20 m sub-grid, it is no longer necessary to remove the outer edges of the 100 m grid to remove interpolation errors.)

6. Gridded 100 m data are saved as 'geotiff' files.
7. These are placed as a transparent layer over a background map using ArcGIS and legends and titles are included. These files are saved as uncompressed jpeg files.

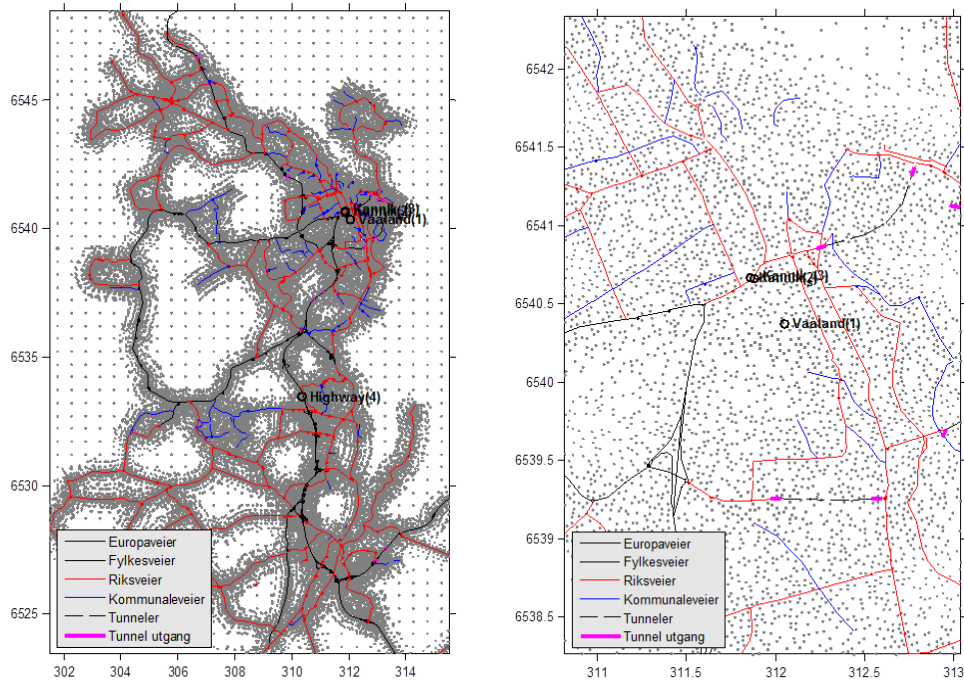


Figure 30: Distribution of mapping receptor points used for mapping in the model domain along with the positions of the measurement sites Kannik and Våland and the highway (E39) receptor site used for emission assessment. Left shows the entire model domain and right a close up in the Stavanger region.

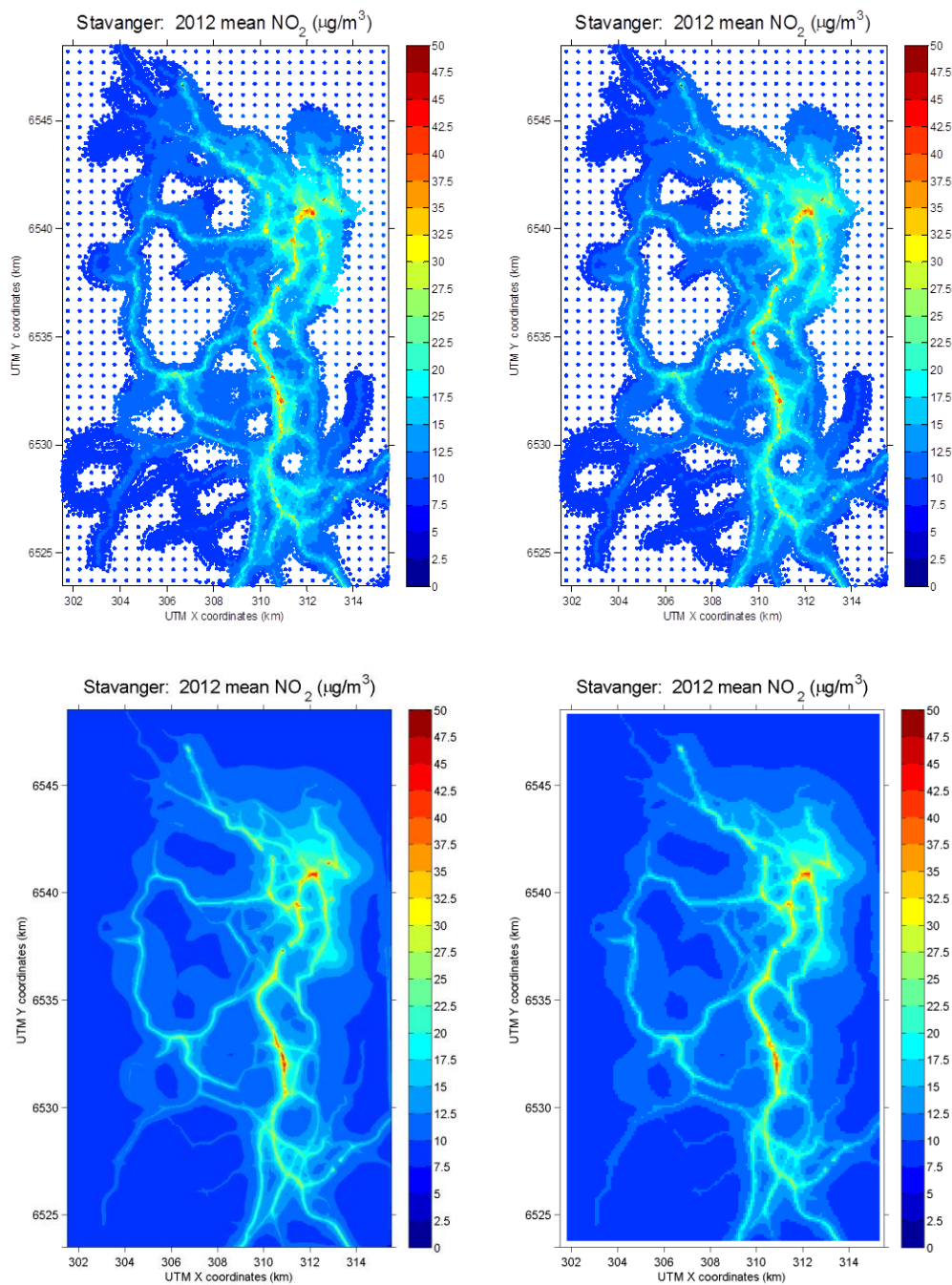


Figure 31: Example of the map making process for annual mean NO_2 . Top left: Receptor point concentrations. Top right: Receptor point concentrations after cubic spline interpolation of the 1 km grid concentrations. Bottom left: Linearly interpolated receptor points to 20 m grids. Bottom right: 100 m grids made from aggregated 20 m grids and with edges removed.

7.2 Final maps of NO₂

The final NO₂ maps are shown in Figure 32 and 33. The calculated maps show the highest concentrations in the Stavanger urban area, particularly along Madlaveien, and also along the motorway E39 between Sandnes and Stavanger in the area near Forus. Along this motorway the highest concentrations are found near intersections. In these two areas the annual mean limit value for NO₂ of 40 µg/m³ is exceeded by 1 - 2 µg/m³. Other urban areas, such as Sandnes, have lower concentrations reflecting the lower traffic volumes along these roads. There are no exceedances in the model region of the hourly mean limit value, i.e. no more than 18 hours > 200 µg/m³.

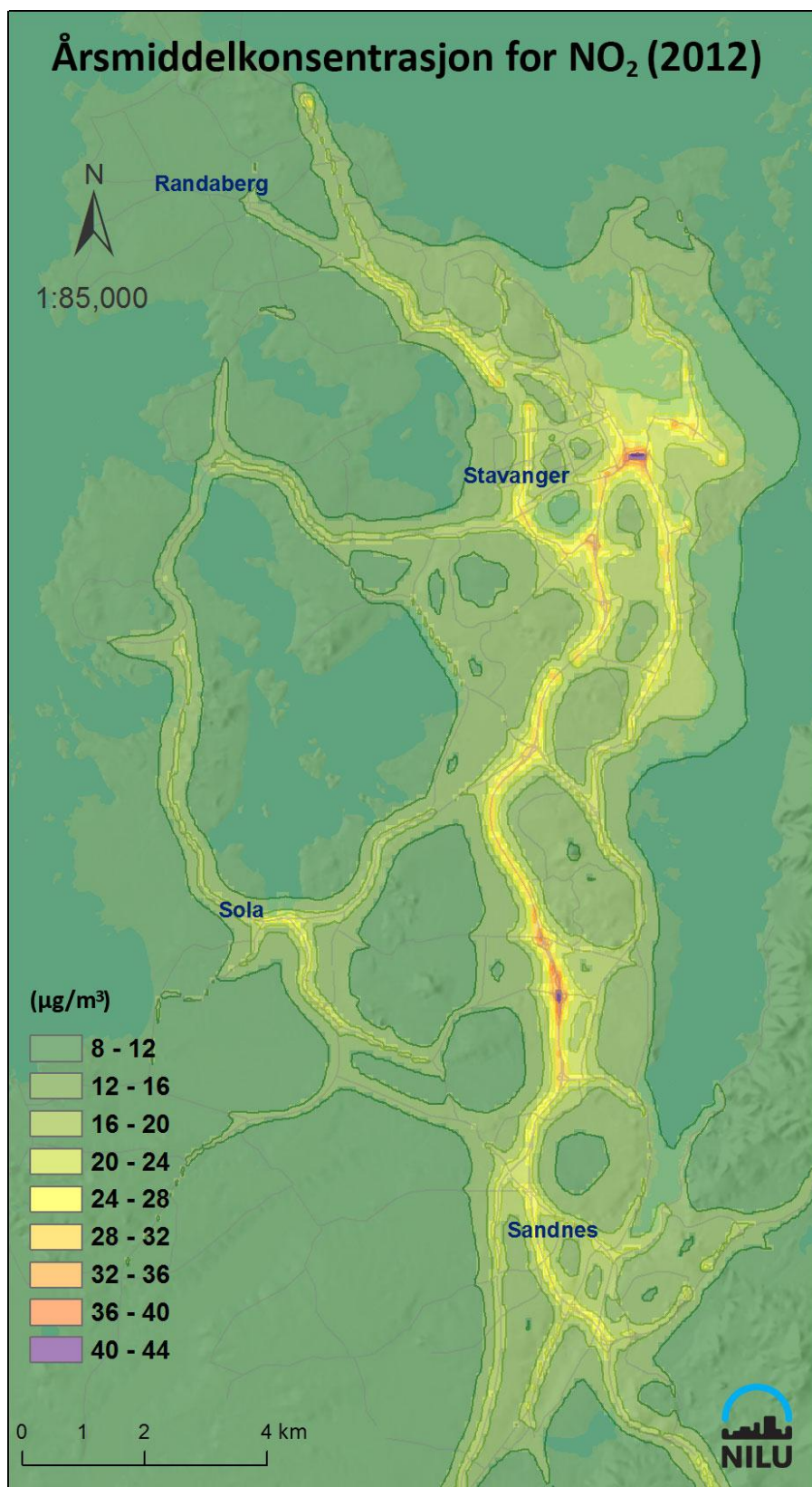


Figure 32: Model calculated annual mean concentrations of NO₂. Concentrations are shown at 100 x 100 m² grid resolution. Contours are added for clarity. Maximum annual mean concentration in the map region is 42.1 µg/m³. The limit value for annual mean NO₂ concentrations is 40 µg/m³.

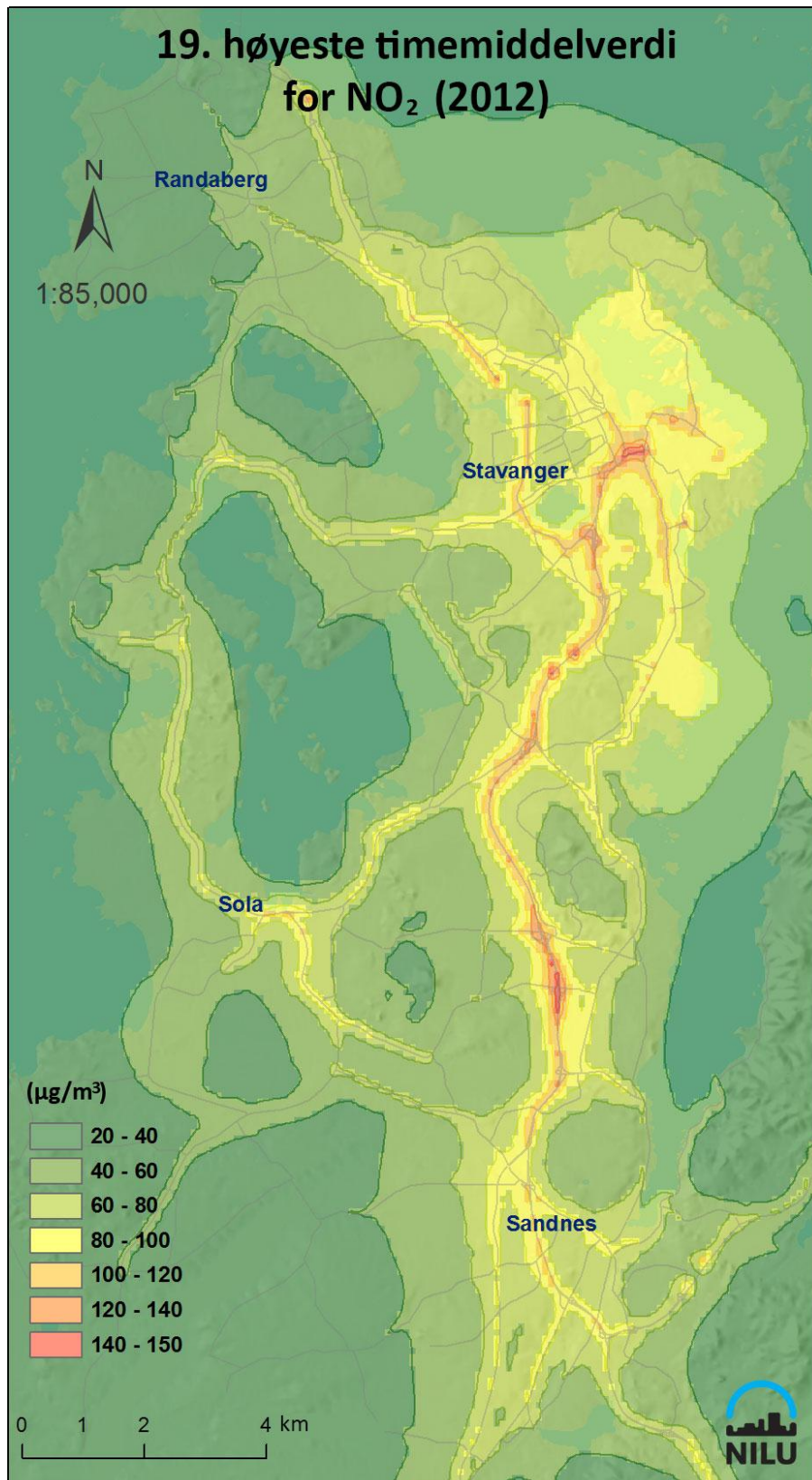


Figure 33. Model calculated 19'th highest hourly mean concentrations of NO₂. Concentrations are shown at 100 x 100 m² grid resolution. Contours are added for clarity. Maximum 19'th highest hourly mean concentration in the map region is 150 µg/m³. The limit value for the 19'th highest hourly mean value is 200 µg/m³.

7.3 Final maps of PM₁₀

Two maps for PM₁₀ are also produced. These are the annual mean concentrations and the 36th highest daily mean concentrations. These are shown in Figure 34 and 35. These maps show highest concentrations along the motorway E39. This is due to road dust emissions. These are highest where there are high traffic volumes and high traffic speeds, since road wear increases with increasing speeds. The maps do not indicate any exceedances of the limit values but, as previously mentioned, there appear to be missing emission sources, at least in the Stavanger urban area. It is not known if these emissions are missing everywhere in the Nord-Jæren region.

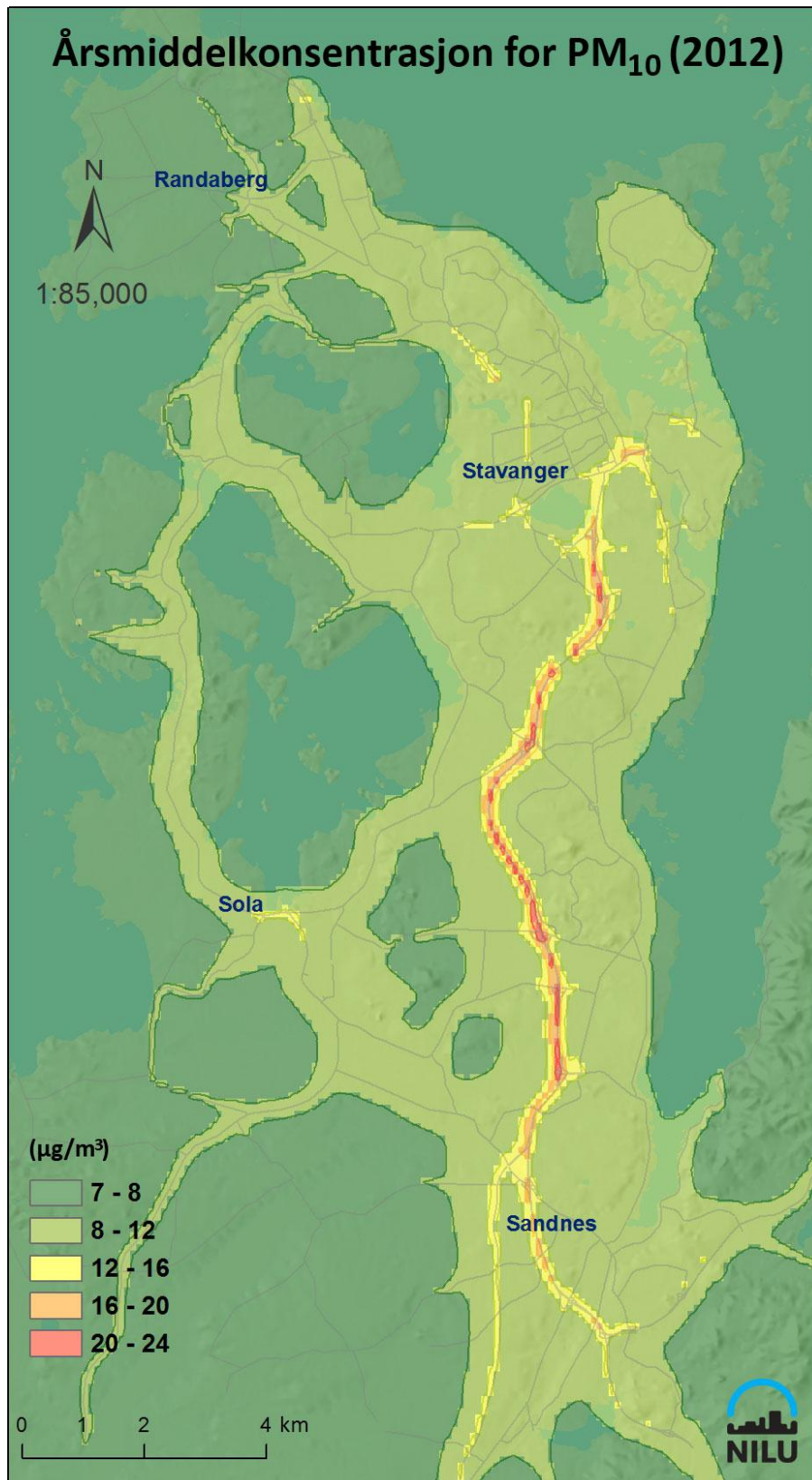


Figure 34. Model calculated annual mean concentrations of PM₁₀. Concentrations are shown at 100 x 100 m² grid resolution. Contours are added for clarity. Maximum annual mean concentration in the map region is 23.5 µg/m³. The limit value for annual mean PM₁₀ concentrations is 40 µg/m³.

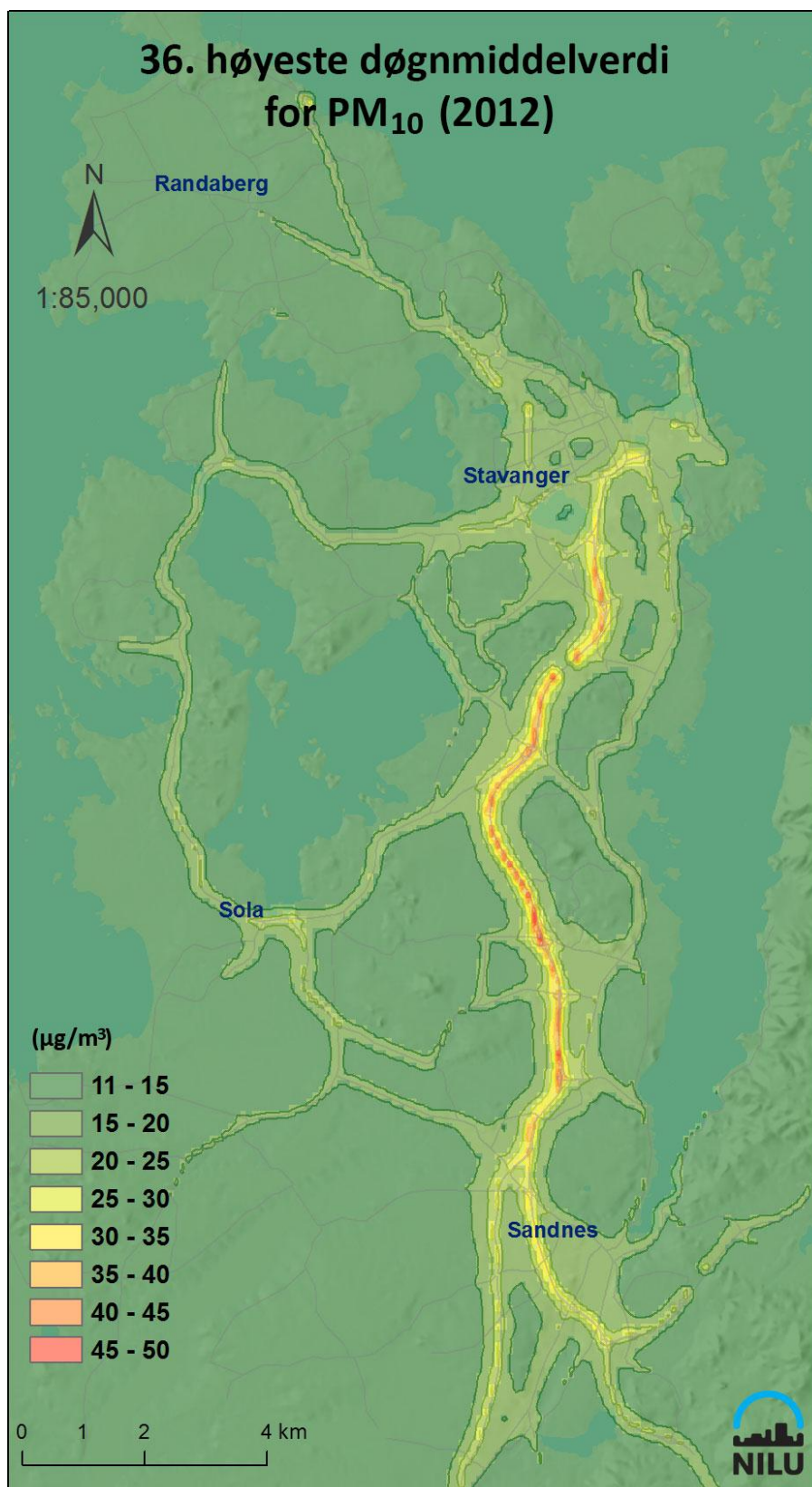


Figure 35. Model calculated 36'th highest daily mean concentrations of PM₁₀. Concentrations are shown at 100 x 100 m² grid resolution. Contours are added for clarity. Maximum 36'th highest daily mean concentration in the map region is 23.5 µg/m³. The limit value for the 36'th highest daily mean concentration is 50 µg/m³.

8 Recommendations and improvements

A number of recommendations and conclusions are given in the summary report. Here we concentrate on the technical aspects in regard to the mapping and list weaknesses and possible future improvements in the modelling and mapping, which will also be relevant for other application areas than just Nord-Jæren.

In general the air quality modelling and mapping has been quite successful for NO_2 , which is strongly associated with traffic emissions. However, the impact of congestion on emissions needs to be better assessed and this can be done by studying traffic counts from the region and updating emission factors appropriately. Other emission sources for NO_x , particularly shipping, should also be reassessed as these may contribute significantly to NO_2 concentrations in some coastal areas. An improvement in the NO_2 chemistry has also been introduced, that accounts for the reaction time of NO with O_3 close to roads. This scheme should be further tested and compared to other observational data.

The PM_{10} modelling indicates, as is often the case, that emissions and/or background levels of PM_{10} are underestimated. There are a large number of sources for PM and though each may be small their accumulative effect becomes significant. For the current application wood burning emissions may be too low and the contribution of other sources, such as sea salt, may be significant. It is not clear why the $\text{PM}_{2.5}$ levels at Kannik and Våland are essentially the same, despite the additional contribution from road traffic at the Kannik site. This similarity is not reflected in the modelling and may instead be the result of an error in the measurements. PM_{10} levels are significantly higher at Kannik but these can be directly contributed to the road dust emissions. The NORTRIP emission model performed very well at this site.

Further to these summary comments we make the following specific notes for future improvements.

8.1 Area emissions

- Reassessment of domestic heating emissions is required. The model indicates that these could be a factor of 2 higher at the measurement stations. This includes both their spatial distribution, currently based on home address density, and their temporal evolution, based on a fixed total emission but allowed to vary due to weekly mean temperatures.
- Reassessment of shipping emissions is required as they appear to be poorly placed and are likely to be quite old. Use of STEAM2 emissions (Jalkanen et al., 2012), as has been carried out in Oslo, can improve both total emissions as well as the spatial distribution. There appears to be significant shipping emissions along the coast outside of the Nord-Jæren peninsula as well, as seen in the MACC-2 regional background maps, though these are not included in the current emissions inventory.
- Previous experience in Oslo have indicated that shipping emissions may be higher and that other combustion sources may be lower due to improvements in technology.

- Other area source contributions, for example agricultural, should be included
- A method for including sea salt emissions should be investigated. This is a major source for PM₁₀ in coastal regions, as can be seen in the MACC-2 regional background maps.
- EPISODE does not include secondary formation of particulates and so relies on regional scale models or regional background observations to provide these data. However, the current method used to calculate regional background, minimum 24 hour concentration measured locally, will never represent this contribution since the minimum will almost always occur during the night when secondary formation is at a minimum.

8.2 Traffic data

- It is not clear how realistic the municipality (kommunal) road traffic counts are, as these are not directly measured. However, this may not be a significant error since the traffic volumes are generally very low for these roads.
- An assessment and adjustment of the traffic congestion and speed parameterisation is required using the available traffic count data from Nord-Jæren.
- The traffic temporal profiles should be updated with observed traffic count data from Nord-Jæren.
- Traffic counts should be made at air quality measurement sites to better understand the local situation.
- In the emission model roads are categorised by their ownership, e.g. 'Fylketsvei' or 'Kommunalevei'. Based on this categorisation temporal profiles, congestion limits and road wear parameters are attributed. This is not a suitable categorisation for a model, which should be based on physical characteristics rather than on ownership.

8.3 NORTRIP modelling

- Good results for the standalone version of NORTRIP were obtained for the station at Kannik along Madlaveien
- The road wear characteristics are unknown but these have been estimated to have wear rates higher than the default value due to the smaller stone sizes used (11 mm rather than 16 mm)
- The NORTRIP model has been applied in a simplified way, calculating road surface moisture for just two types of roads. This means that the model calculations do not include removal processes due to spray and do not include salt emissions. This may result in an overestimate of PM₁₀ emissions for higher speed motorways where spray removal becomes significant. The model needs to be further developed to calculate road moisture for each individual road so that all processes can be included. .

8.4 NO₂ chemistry parameterisation

- The introduction of the near road NO₂ chemistry parameterisation is an improvement on the current photo-stationary assumption

- Further development and testing is required to assure its validity and its use in other model applications

8.5 Mapping

- The mapping methodology provides a significant improvement on maps currently made using AirQUIS. The method should be further optimised and developed for its wider use in other applications.

8.6 Meteorology

- Meteorological data should be measured at air quality sites allowing for a better interpretation of the air quality measurements
- If possible in the future, meteorological measurements from a more centrally located mast, e.g. in Stavanger, should be used.
- The combined use of modelled (forecasting) and observed meteorology should improve the meteorological fields significantly and is recommended for further applications

8.7 Air quality measurements

- Use of passive samplers for NO₂ can give important spatial information on concentrations and provide validation for the model calculations. A large number of these samplers can be distributed throughout the region for limited periods at low cost.
- In order to assess the contribution of salt (sea or road) in the region analysis can be made of filter samples to determine salt contributions.
- In order to better understand why PM_{2.5} has similar levels at both the Kannik and Våland stations an analysis of these data, also for other years, is recommended.
- It is recommended that a suitable regional background air quality station be deployed. This will provide the necessary information concerning the local versus regional contribution and will reduce uncertainty in the air quality source contributions significantly.

9 References

- Bedre byluft (2013) Luftkvaliteten i Norge. **URL:** www.luftkvalitet.info/home/forecast.aspx [Downloaded 18 December 2013].
- Denby, B.R., Sundvor, I. (2012) NORTRIP model development and documentation: NO_x-exhaust Road TRAffic Induced Particle emission modelling. Kjeller, NILU (NILU OR, 23/2012).
- Denby, B.R., Sundvor, I. (2013) Modelling non-exhaust emissions of PM₁₀ in Oslo: Impact of the environmental speed limit using the NORTRIP model. Kjeller, NILU (NILU OR, 41/2013).
- Denby, B.R., Sundvor, I., Johansson, C., Pirjola, L., Ketzel, M., Norman, M., Kupiainen, K., Gustafsson, M., Blomqvist, G., Kauhaniemi, M., Omstedt, G. (2013a) A coupled road dust and surface moisture model to predict non-exhaust road traffic induced particle emissions (NORTRIP). Part 2: surface moisture and salt impact modelling. *Atmos. Environ.*, *81*, 485-503. doi:10.1016/j.atmosenv.2013.09.003
- Denby, B.R., Sundvor, I., Johansson, C., Pirjola, L., Ketzel, M., Norman, M., Kupiainen, K., Gustafsson, M., Blomqvist, G., Omstedt, G. (2013b) A coupled road dust and surface moisture model to predict non-exhaust road traffic induced particle emissions (NORTRIP). Part 1: road dust loading and suspension modelling. *Atmos. Environ.*, *77*, 283-300. doi:10.1016/j.atmosenv.2013.04.069.
- Jalkanen, J.P., Johansson, L., Kukkonen, J., Brink, A., Kalli, J., Stipa, T. (2012) Extension of an assessment model of ship traffic exhaust emissions for particulate matter and carbon monoxide. *Atmos. Chem. Phys.*, *12*, 2641-2659. doi:10.5194/acp-12-2641-2012.
- MACC (2013) MACC: Monitoring Atmospheric Composition and Climate. European Air Quality Monitoring and Forecasting web site. **URL:** www.gmes-atmosphere.eu/services/raq/raq_nrt/ [Downloaded 10 January 2014].
- OFV (2013) Kjøretøystatistikk 2013. Oslo, Opplysningsrådet for veitrafikken.
- Slørdal, L.H., Walker, S.E., Solberg, S. (2003) The urban air dispersion model EPISODE applied in AirQUIS2003. Technical description. Kjeller, NILU (NILU TR, 12/2003).
- Stavanger kommune (2013) Luftkvalitet Stavanger, årsrapport 2012. Stavanger kommune, avdeling for miljørettet helsevern.
- Statens vegvesen (2013) Nasjonal vegdatabank (NVDB). **URL:** <http://www.vegvesen.no/Fag/Teknologi/Nasjonal+vegdatabank> [Downloaded 18 December 2013].

Ødegaard, V., Gjerstad, K.I., Slørdal, L.H., Abildsnes, H., Olsen, T. (2013) Bedre byluft. Prognoser for meteorologi og luftkvalitet i norske byer vinteren 2011 - 2012. Oslo, Meteorologisk institutt (met.no report, 10/2013).



**Norwegian Institute
for Air Research**

NILU – Norwegian Institute for Air Research
P.O. Box 100, N-2027 Kjeller, Norway
Associated with CIENS and the Fram Centre
ISO certified according to NS-EN ISO 9001/ISO 14001

REPORT SERIES OPPDRAGRSRAPPORT	REPORT NO. TR 1/2014	ISBN: 978-82-425-2643-4 (print) 978-82-425-2644-1 (electronic) ISSN: 0807-7185	
DATE 25/02/2014	SIGN. 	ANT. SIDER 52	PRIS NOK 150.-
TITLE Air quality maps of NO ₂ and PM ₁₀ for the region including Stavanger, Sandnes, Randaberg and Sola (Nord-Jæren) Documentation of methodology		PROJECT LEADER Bruce Rolstad Denby	
		NILU PROJECT NO. O-113137	
AUTHOR(S) Bruce Rolstad Denby, Ingrid Sundvor, Philipp Schneider, Dam Vo Thanh		CLASSIFICATION * A	
		CONTRACT REF.	
QUALITY CONTROLLER: Leiv Håvard Slørdal			
REPORT PREPARED FOR Statens vegvesen Region vest, Samfunnsseksjonen Askedalen 4 6863 Leikanger			
ABSTRACT. This report documents the methodology used to make air quality maps of NO ₂ and PM ₁₀ for the region Nord-Jæren, which includes the municipalities of Stavanger, Sandnes, Randaberg and Sola. It provides support documentation for the summary report OR 57/2013			
NORWEGIAN TITLE Luftkvalitetskart for NO ₂ og PM ₁₀ for Stavanger-regionene, inkludert Stavanger, Sandnes, Randaberg og Sola (Nord-Jæren). Dokumentasjon av metodikker brukt.			
KEYWORDS Air quality	Urban traffic pollution		
REFERAT. Denne rapporten dokumenterer metodikken som har blitt brukt for å lage luftkvalitetskart av NO ₂ og PM ₁₀ for området Nord-Jæren, som innbefatter kommunene Stavanger, Sandnes, Randaberg og Sola. Denne rapport støtter oppsummeringsrapporten NILU OR 57/2013			

* Kategorier A Åpen – kan bestilles fra NILU
 B Begrenset distribusjon
 C Kan ikke utleveres

REFERENCE: O-113137
DATE: FEBRUARY 2014
ISBN: 978-82-425-2643-4 (print)
978-82-425-2644-1 (electronic)

NILU – Norwegian Institute for Air Research is an independent, nonprofit institution established in 1969. Through its research NILU increases the understanding of climate change, of the composition of the atmosphere, of air quality and of hazardous substances. Based on its research, NILU markets integrated services and products within analyzing, monitoring and consulting. NILU is concerned with increasing public awareness about climate change and environmental pollution.